Non-linear Evolution of Matter Power Spectrum in Modified Theory of Gravity

Kazuya Koyama[1], Atsushi Taruya[2,3], Takashi Hiramatsu[4]

[1] *Institute of Cosmology & Gravitation, University of Portsmouth, Portsmouth, Hampshire, PO1 2EG, UK*

[2] *Research Center for the Early Universe, School of Science, University of Tokyo, Bunkyo-ku, Tokyo 113-0033, Japan*

[3] *Institute for the Physics and Mathematics of the Universe, University of Tokyo, Kashiwa, Chiba 277-8568, Japan and*

[4] *Institute for Cosmic Ray Research, University of Tokyo, Kashiwa, Chiba 277-8582, Japan*

(Dated: today)

We present a formalism to calculate the non-linear matter power spectrum in modified gravity models that explain the late-time acceleration of the Universe without dark energy. Any successful modified gravity models should contain a mechanism to recover General Relativity (GR) on small scales in order to avoid the stringent constrains on deviations from GR at solar system scales. Based on our formalism, the quasi non-linear power spectrum in the Dvali-Gabadadze-Porratti (DGP) braneworld models and $f(R)$ gravity models are derived by taking into account the mechanism to recover GR properly. We also extrapolate our predictions to fully non-linear scales using the Parametrized Post Friedmann (PPF) framework. In DGP and $f(R)$ gravity models, the predicted non-linear power spectrum is shown to reproduce N-body results. We find that the mechanism to recover GR suppresses the difference between the modified gravity models and dark energy models with the same expansion history, but the difference remains large at weakly non-linear regime in these models. Our formalism is applicable to a wide variety of modified gravity models and it is ready to use once consistent models for modified gravity are developed.

PACS numbers: 98.80.-k

I. INTRODUCTION

The late-time acceleration of the Universe is surely the most challenging problem in cosmology. Within the framework of general relativity (GR), the acceleration originates from dark energy. The simplest option is the cosmological constant. However, in order to explain the current acceleration of the Universe, the required value of the cosmological constant must be incredibly small. Alternatively, there could be no dark energy, but a large distance modification of GR may account for the late-time acceleration of the Universe. Recently considerable efforts have been made to construct models for modified gravity as an alternative to dark energy and distinguish them from dark energy models by observations (see [1, 2, 3, 4] for reviews).

Although fully consistent models have not been constructed yet, some indications of the nature of the modified gravity models have been obtained. In general, there are three regimes of gravity in modified gravity models [2, 5]. On the largest scales, gravity must be modified significantly in order to explain the late time acceleration without introducing dark energy. On the smallest scales, the theory must approach GR because there exist stringent constraints on the deviation from GR at solar system scales. On intermediate scales between the cosmological horizon scales and the solar system scales, there can be still a deviation from GR. In fact, it is a very common feature in modified gravity models that there is a significant deviation from GR on large scale structure scales. This is due to the fact that, once we modify GR, there arises a new scalar degree of freedom in gravity. This scalar mode changes gravity even below the length scale where the modification of the tensor sector of gravity becomes significant, which causes the cosmic acceleration.

Therefore, large scale structure of the Universe offers the best opportunity to distinguish between modified gravity models and dark energy models in GR [6, 7, 8, 9, 10, 11, 12, 13, 14, 15, 16, 17, 18, 19, 20, 21, 22]. The expansion history of the Universe determined by the Friedman equation can be completely the same in modified gravity models and dark energy models. In fact, it is always possible to find a dark energy model that can mimic the expansion history of the Universe in a given modified gravity model by tuning the equation of state of dark energy. However, this degeneracy can be broken by the growth rate of structure formation. This is because the scalar degree of freedom in modified gravity models changes the strength of gravity on sub-horizon scales and thus changes the growth rate of structure formation. Thus combining the geometrical test and structure formation test, one can distinguish between dark energy models and modified gravity models.

However, there is a subtlety in testing modified gravity models using large scale structure of the Universe. In any successful modified gravity models, we should recover GR on small scales. Indeed, unless there is an additional mechanism to screen the scalar interaction which changes the growth rate of structure formation, the modification of gravity contradicts to the stringent constraints on the deviation from GR at solar system scales. This mechanism affects the non-linear clustering of dark matter. We expect that the power-spectrum of dark matter perturbations approaches the one in the GR dark energy model with the same expansion history of the Universe because the modification of gravity disappears on small scales. Then the difference between a modified gravity model and a dark energy model with the same expansion history becomes smaller on smaller scales. This recovery of GR has important implications for weak lensing measurements because the strongest signals in weak lensing measurements come from non-linear scales. We should note that the non-linear power spectrum is also sensitive to the properties of dark energy [23].

In almost all of the literature, the non-linear power spectrum in modified gravity models was derived using the mapping formula between the linear power spectrum and the non-linear power spectrum. This is equivalent to assume that gravity is modified down to small scales in the same way as in the linear regime which contradicts to the solar system constraints. Thus this approach overestimates the difference between modified gravity models and dark energy models. This was explicitly shown by N-body simulations in the context of $f(R)$ gravity [24, 25, 26]. In $f(R)$ gravity, the Einstein-Hilbert action is replaced by an arbitrary function of Ricci curvature (see [27, 28] for a review). This model is equivalent with the Brans-Dicke (BD) theory with non-trivial potential [29, 30, 31]. The BD scalar mediates an additional gravitational interaction that enhances the gravitational force below the Compton wavelength of the BD scalar. If the mass of the BD scalar becomes larger in a dense environment like in the solar system, the Compton wavelength becomes short and we can recover GR. This is known as the chameleon mechanism [32]. In the context of $f(R)$ gravity, by tuning the function f, it is possible to make the Compton wavelength of the BD scalar short at solar system scales and screen the BD scalar interaction [33, 34, 35, 36]. N-body simulations show that, due to this mechanism, the deviation of the non-linear power spectrum from GR is suppressed on small scales [24, 25, 26]. It was shown that the mapping formula failed to describe this recovery of GR and it overestimated the deviation from GR.

In this paper, we develop a formalism to treat the quasi non-linear evolution of the power spectrum in modified gravity models by properly taking into account the mechanism to recover GR on small scales. Our formalism is based on the closure approximation which gives a closed set of evolution equations for the matter power spectrum [37]. These evolution equations reproduce the one-loop results of the standard perturbation theory (SPT) by replacing the quantities in the non-linear terms with linear-order ones. The SPT in GR is tested against N-body simulations extensively recently and it has been shown that, at the quasi non-linear regime, it can predict the power-spectrum with a sub-percent accuracy [38]. Although the validity regime of the perturbation theory is limited, it is the most relevant regime to distinguish between modified gravity models and dark energy models in GR because the difference in the two models is large in the linear and quasi-non-linear regime. We developed a general formalism which can be applied to many modified gravity models including well studied models such as $f(R)$ gravity and braneworld models.

This paper is organized as follows. In section II, we introduce effective equation for quasi-static perturbations to describe the Newtonian limit of gravity. Basic equations which are necessary to compute the power spectrum are presented in section III. In section IV, the non-linear evolution equations of the power spectrum are derived based on the closure approximation proposed by Ref. [37]. The closure approximation is one of the non-perturbative prescriptions for comupting non-linear power spectrum, and it is shown to be equivalent to the one-loop level of renormalized perturbation theory by Crocce and Scoccimarro [39] and the 2PI effective action method by Valageas [40]. By replacing all the quantities in non-linear terms with linear-order ones, the so-called one-loop power spectrum is obtained numerically which describes the leading-order non-linear corrections. In section V, we apply this formalism to Dvali-Gabadadze-Porratti (DGP) braneworld models. In the case of DGP models, we can derive the quasi non-linear power spectrum analytically. We test our numerical code to solve the closure equation against the analytical results. The quasi non-linear spectrum is derived also in $f(R)$ gravity models. In this case, our results are compared with N-body simulations. In section VI, we apply the Parametrized post-Friedman (PPF) framework to predict the fully non-linear power spectrum. Using the solutions in the perturbation theory, we determine a parameter in the PPF framework. Then we predict the non-linear power spectrum by extrapolating this parameter to fully non-linear scales. The predictions of the PPF formalism are compared with N-body simulations. Section VII is devoted to conclusions. In appendix A, a numerical scheme to solve the closure equations is presented. In appendix B, we derive the quasi non-linear power spectrum in DGP models analytically.

II. QUASI-STATIC PERTURBATIONS IN MODIFIED GRAVITY MODELS

We consider perturbations around the Friedman-Robertson-Walker universe described in the Newtonian gauge:

$$ds^2 = -(1+2\psi)dt^2 + a^2(1+2\phi)\delta_{ij}dx^i dx^j. \tag{2.1}$$

We will study the evolution of matter fluctuations inside the Hubble horizon. Then we can use the quasi-static approximation and neglect the time derivatives of the perturbed quantities compared with the spatial derivatives. As mentioned in the introduction, the large distance modification of gravity, which is necessary to explain the late-time acceleration, generally modifies gravity even on sub-horizon scales due to the introduction of a new scalar degree of freedom. This modification of gravity due to the scalar mode can be described by Brans-Dicke (BD) gravity. Under the quasi-static approximations, perturbed modified Einstein equations give

$$\phi + \psi = -\varphi, \tag{2.2}$$

$$\frac{1}{a^2}\nabla^2\psi = 4\pi G\rho_m\delta - \frac{1}{2a^2}\nabla^2\varphi, \tag{2.3}$$

$$(3+2\omega_{\rm BD})\frac{1}{a^2}\nabla^2\varphi = -8\pi G\rho_m\delta, \tag{2.4}$$

where G is the Newton constant measured in Cavendish-like experiments, ρ_m is the background dark matter energy density and δ is dark matter density perturbations. Under the quasi-static approximations $\omega_{\rm BD}$ can be any function of time. In general, modified gravity models that explain the late time acceleration predict $\omega_{\rm BD} \sim O(1)$ on sub-horizon scales today. This would contradict to the solar system constraints which require $\omega_{\rm BD} > 40000$. However, this constraint can be applied only when the BD scalar has no potential and no self-interactions. Thus, in order to avoid this constraint, the BD scalar should acquire some interaction terms on small scales. In general we expect that the BD scalar field equation is given by

$$(3+2\omega_{\rm BD})\frac{1}{a^2}k^2\varphi = 8\pi G\rho_m\delta - \mathcal{I}(\varphi), \tag{2.5}$$

in a Fourier space. Here the interaction term $\mathcal{I}$ can be expanded as

$$\begin{aligned}\mathcal{I}(\varphi) &= M_1(k)\varphi + \frac{1}{2}\int\frac{d^3\boldsymbol{k}_1 d^3\boldsymbol{k}_2}{(2\pi)^3}\delta_D(\boldsymbol{k}-\boldsymbol{k}_{12})M_2(\boldsymbol{k}_1,\boldsymbol{k}_2)\varphi(\boldsymbol{k}_1)\varphi(\boldsymbol{k}_2)\\ &+\frac{1}{6}\int\frac{d^3\boldsymbol{k}_1 d^3\boldsymbol{k}_2 d^3\boldsymbol{k}_3}{(2\pi)^6}\delta_D(\boldsymbol{k}-\boldsymbol{k}_{123})M_3(\boldsymbol{k}_1,\boldsymbol{k}_2,\boldsymbol{k}_3)\varphi(\boldsymbol{k}_1)\varphi(\boldsymbol{k}_2)\varphi(\boldsymbol{k}_3)+...\end{aligned} \tag{2.6}$$

where $\boldsymbol{k}_{ij} = \boldsymbol{k}_i + \boldsymbol{k}_j$ and $\boldsymbol{k}_{ijk} = \boldsymbol{k}_i + \boldsymbol{k}_j + \boldsymbol{k}_k$.

We should emphasize that effective equations (2.2), (2.3) and (2.5) in the BD theory can be applied only to quasi-static perturbations. We allow the time dependence of the BD parameter in these effective equations but this does not necessarily mean that we are considering scalar tensor theory where the BD parameter is a function of the BD scalar. The effective equations are applicable to scalar tensor theory by adding appropriate non-linear interaction terms in $\mathcal{I}$. Although this is an interesting possibility (see [41, 42, 43] for the analysis of perturbations in scalar tensor theory), we will not consider this possibility in this paper. We also note that a general parametrization of linear perturbations in modified gravity was developed in [44] and a similar parametrisation of quasi-static perturbations to ours was considered at linearized level in [21].

In this paper, we consider two known mechanisms where the non-linear interaction terms $\mathcal{I}$ are responsible for the recovery of GR on small scales. There are other possibilities to recover GR on small scales for example by decoupling baryons, but we focus on the following two possibilities in this paper. One is the chameleon mechanism [32]. In this case, the BD scalar has a non-trivial potential, and acquires a mass. Then, the BD scalar mediates the Yukawa-type force and the interaction decays exponentially above the length scale determined by the inverse of the mass, the Compton wavelength. Because of this, the scalar interaction is hidden above the Compton wavelength, and GR is recovered. The BD scalar is coupled to the trace of the energy momentum tensor. Thus the effective potential depends on the energy density of the environment. The potential is tuned so that the mass of the BD scalar becomes large for a dense environment such as the solar system. In order for the chameleon mechanism to work, the scalar fields needs a runaway potential to be efficient [32]. Then the Compton wavelength becomes very short for a dense environment and the scalar mode is effectively hidden. In this paper, we deal with this mechanism perturbatively. M_1 determines the mass term in the cosmological background. The higher order terms $M_i, (i > 1)$ describe the change of the mass term due to the change of the energy density. If the chameleon mechanism is at work, the effective mass becomes larger when the density fluctuations become non-linear.

The other mechanism relies on the existence of the non-linear derivative interactions. A typical example is the Dvali-Gabadadze-Porratti (DGP) braneworld model where we are supposed to be living on a 4D brane in a 5D Minkowski spacetime [45]. In this model, the BD scalar is identified as the brane bending mode which describes the deformation of the 4D brane in the 5D bulk spacetime. The brane bending mode has a large second-order term in the equation of motion which cannot be neglected even when the metric perturbations remain linear. This corresponds to

the existence of a large $M_2(k)$ term [46, 47, 48]. It has been shown that once this second order term dominates over the linear term, the scalar mode is hidden and the solutions for metric perturbations approach GR solutions. For a static spherically symmetric source, we can identify the length scale below which the second order interaction becomes important. This length scale is known as the Vainshtein radius [49]. In the cosmological situation, it is expected that once the density perturbations become non-linear, the second order term becomes important and we recover GR. In the next section, we apply the perturbation theory to solve the equations (2.2), (2.3) and (2.5). Thus we only keep up to the third order in the expansion of $\mathcal{I}$ which is necessary to calculate the quasi non-linear power spectrum.

The evolution equations for matter perturbations are obtained from the conservation of energy momentum tensor, the continuity equation and the Euler equation:

$$\frac{\partial\delta}{\partial t}+\frac{1}{a}\nabla\cdot[(1+\delta)\boldsymbol{v}]=0, \tag{2.7}$$

$$\frac{\partial\boldsymbol{v}}{\partial t}+H\boldsymbol{v}+\frac{1}{a}(\boldsymbol{v}\cdot\nabla)\boldsymbol{v}=-\frac{1}{a}\nabla\psi. \tag{2.8}$$

Eqs. (2.3), (2.5), (2.7) and (2.8) are the basic equations that have to be solved. In the next section, we derive evolution equation for perturbations in a compact form.

III. EVOLUTION EQUATIONS FOR PERTURBATIONS

Assuming the irrotationality of fluid quantities, the velocity field $\boldsymbol{v}$ is expressed in terms of velocity divergence $\theta\equiv\nabla\cdot\boldsymbol{v}/(a\,H)$. Then the Fourier transform of the fluid equations (2.7) and (2.8) become

$$H^{-1}\frac{\partial\delta(\boldsymbol{k})}{\partial t}+\theta(\boldsymbol{k})=-\int\frac{d^3\boldsymbol{k}_1d^3\boldsymbol{k}_2}{(2\pi)^3}\delta_{\rm D}(\boldsymbol{k}-\boldsymbol{k}_1-\boldsymbol{k}_2)\alpha(\boldsymbol{k}_1,\boldsymbol{k}_2)\,\theta(\boldsymbol{k}_1)\delta(\boldsymbol{k}_2), \tag{3.1}$$

$$H^{-1}\frac{\partial\theta(\boldsymbol{k})}{\partial t}+\left(2+\frac{\dot H}{H^2}\right)\theta(\boldsymbol{k})-\left(\frac{k}{a\,H}\right)^2\psi(\boldsymbol{k})=-\frac{1}{2}\int\frac{d^3\boldsymbol{k}_1d^3\boldsymbol{k}_2}{(2\pi)^3}\delta_{\rm D}(\boldsymbol{k}-\boldsymbol{k}_1-\boldsymbol{k}_2)\beta(\boldsymbol{k}_1,\boldsymbol{k}_2)\,\theta(\boldsymbol{k}_1)\theta(\boldsymbol{k}_2), \tag{3.2}$$

where the kernels in the Fourier integrals, α and β, are given by

$$\alpha(\boldsymbol{k}_1,\boldsymbol{k}_2)=1+\frac{\boldsymbol{k}_1\cdot\boldsymbol{k}_2}{|\boldsymbol{k}_1|^2},\qquad\beta(\boldsymbol{k}_1,\boldsymbol{k}_2)=\frac{(\boldsymbol{k}_1\cdot\boldsymbol{k}_2)\,|\boldsymbol{k}_1+\boldsymbol{k}_2|^2}{|\boldsymbol{k}_1|^2|\boldsymbol{k}_2|^2}. \tag{3.3}$$

As for the Poisson equation (2.3), the potential ψ is couples to δ through the BD scalar φ in a fully non-linear way due to the interaction term $\mathcal{I}$. To derive closed equations for δ and θ, we must employ the perturbative approach to Eq. (2.5). By solving Eq. (2.5) perturbatively assuming $\varphi<1$, ψ can be expressed in terms of δ as

$$-\left(\frac{k}{a}\right)^2\psi=\frac{1}{2}\,\kappa^2\,\rho_m\,\left[1+\frac{1}{3}\frac{(k/a)^2}{\Pi(k)}\right]\,\delta(\boldsymbol{k})+\frac{1}{2}\left(\frac{k}{a}\right)^2\,S(\boldsymbol{k}), \tag{3.4}$$

where

$$\Pi(k)=\frac{1}{3}\left((3+2\omega_{\rm BD})\frac{k^2}{a^2}+M_1\right), \tag{3.5}$$

and $\kappa^2=8\pi G$. The function $S(\boldsymbol{k})$ is the non-linear source term which is obtained perturbatively using (2.3) as

$$\begin{aligned}S(\boldsymbol{k}) \;=\; & -\frac{1}{6\Pi(\boldsymbol{k})}\left(\frac{\kappa^2\,\rho_m}{3}\right)^2\int\frac{d^3\boldsymbol{k}_1d^3\boldsymbol{k}_2}{(2\pi)^3}\,\delta_{\rm D}(\boldsymbol{k}-\boldsymbol{k}_{12})M_2(\boldsymbol{k}_1,\boldsymbol{k}_2)\frac{\delta(\boldsymbol{k}_1)\,\delta(\boldsymbol{k}_2)}{\Pi(\boldsymbol{k}_1)\Pi(\boldsymbol{k}_2)}\\ & -\frac{1}{18\,\Pi(\boldsymbol{k})}\left(\frac{\kappa^2\,\rho_m}{3}\right)^3\int\frac{d^3\boldsymbol{k}_1d^3\boldsymbol{k}_2d^3\boldsymbol{k}_3}{(2\pi)^6}\delta_{\rm D}(\boldsymbol{k}-\boldsymbol{k}_{123})\left\{M_3(\boldsymbol{k}_1,\boldsymbol{k}_2,\boldsymbol{k}_3)-\frac{M_2(\boldsymbol{k}_1,\boldsymbol{k}_2+\boldsymbol{k}_3)M_2(\boldsymbol{k}_2,\boldsymbol{k}_3)}{\Pi(\boldsymbol{k}_{23})}\right\}\\ & \times\frac{\delta(\boldsymbol{k}_1)\,\delta(\boldsymbol{k}_2)\delta(\boldsymbol{k}_3)}{\Pi(\boldsymbol{k}_1)\Pi(\boldsymbol{k}_2)\Pi(\boldsymbol{k}_3)}.\end{aligned} \tag{3.6}$$

The expression (3.6) is valid up to the third-order in δ.

The perturbation equations (3.1), (3.2) and (3.4) can be further reduced to a compact form by introducing the following quantity:

$$\Phi_a(\boldsymbol{k}) = \begin{pmatrix} \delta(\boldsymbol{k}) \\ -\theta(\boldsymbol{k}) \end{pmatrix}. \tag{3.7}$$

We can write down the basic equations in a single form as

$$\frac{\partial \Phi_a(\boldsymbol{k};\tau)}{\partial \tau} + \Omega_{ab}(k;\tau)\,\Phi_b(\boldsymbol{k};\tau) = \int \frac{d^3\boldsymbol{k}_1 d^3\boldsymbol{k}_2}{(2\pi)^3}\,\delta_{\rm D}(\boldsymbol{k}-\boldsymbol{k}_{12})\,\gamma_{abc}(\boldsymbol{k}_1,\boldsymbol{k}_2;\tau)\,\Phi_b(\boldsymbol{k}_1;\tau)\Phi_c(\boldsymbol{k}_2;\tau) + \int \frac{d^3\boldsymbol{k}_1 d^3\boldsymbol{k}_2 d^3\boldsymbol{k}_3}{(2\pi)^6}\,\delta_{\rm D}(\boldsymbol{k}-\boldsymbol{k}_{123})\,\sigma_{abcd}(\boldsymbol{k}_1,\boldsymbol{k}_2,\boldsymbol{k}_3;\tau)\,\Phi_b(\boldsymbol{k}_1;\tau)\Phi_c(\boldsymbol{k}_2\tau)\Phi_d(\boldsymbol{k}_3;\tau), \tag{3.8}$$

where the time variable τ is defined by $\tau = \ln a(t)$. The matrix Ω_{ab} is given by

$$\Omega_{ab}(k;\tau) = \begin{pmatrix} 0 & -1 \\ -\dfrac{\kappa^2}{2}\dfrac{\rho_m}{H^2}\left[1+\dfrac{1}{3}\dfrac{(k/a)^2}{\Pi(k)}\right] & 2+\dfrac{\dot H}{H^2} \end{pmatrix}. \tag{3.9}$$

From the $(2,1)$ component of Ω_{ab}, we can define the effective Newton constant as

$$G_{\rm eff} = G\left[1+\frac{1}{3}\frac{(k/a)^2}{\Pi(k)}\right]. \tag{3.10}$$

If M_1=0, the effective Newton constant is given by

$$G_{\rm eff} = \frac{2(2+\omega_{\rm BD})}{3+2\omega_{\rm BD}}G. \tag{3.11}$$

See Ref. [50] for a review on the BD theory. For a positive $\omega_{\rm BD} > 0$, the effective gravitational constant is larger than GR and the gravitational force is enhanced. On the other hand, if $M_1 \gg k^2/a^2$, $G_{\rm eff}$ becomes G. The quantity γ_{abc} is the vertex function as in the GR case, but new non-vanishing components arise in the case of modified gravity:

$$\gamma_{abc}(\boldsymbol{k}_1,\boldsymbol{k}_2;\tau) = \begin{cases} \dfrac{1}{2}\,\alpha(\boldsymbol{k}_2,\boldsymbol{k}_1) & ;\ (a,b,c)=(1,1,2), \\ \dfrac{1}{2}\,\alpha(\boldsymbol{k}_1,\boldsymbol{k}_2) & ;\ (a,b,c)=(1,2,1), \\ -\dfrac{1}{12H^2}\left(\dfrac{\kappa^2\,\rho_m}{3}\right)^2\left(\dfrac{k_{12}^2}{a^2}\right)\dfrac{M_2(\boldsymbol{k}_1,\boldsymbol{k}_2)}{\Pi(\boldsymbol{k}_{12})\Pi(\boldsymbol{k}_1)\Pi(\boldsymbol{k}_2)} & ;\ (a,b,c)=(2,1,1), \\ \dfrac{1}{2}\,\beta(\boldsymbol{k}_1,\boldsymbol{k}_2) & ;\ (a,b,c)=(2,2,2), \\ 0 & ;\ \text{otherwise}. \end{cases} \tag{3.12}$$

Here γ_{211} is absent in GR. Note that the symmetric properties of the vertex function, $\gamma_{abc}(\boldsymbol{k}_1,\boldsymbol{k}_2;\tau) = \gamma_{acb}(\boldsymbol{k}_2,\boldsymbol{k}_1;\tau)$, still hold in the modified theory of gravity. In Eq. (3.8), there appears another vertex function coming from the non-linearity of Poisson equation. The explicit form of the higher-order vertex function σ_{abcd} is given by

$$\sigma_{abcd}(\boldsymbol{k}_1,\boldsymbol{k}_2,\boldsymbol{k}_3;\tau) = \begin{cases} -\dfrac{1}{36H^2}\left(\dfrac{\kappa^2\rho_m}{3}\right)^3\left(\dfrac{k_{123}^2}{a^2}\right)\dfrac{M_3(\boldsymbol{k}_1,\boldsymbol{k}_2,\boldsymbol{k}_3)}{\Pi(\boldsymbol{k}_{123})\Pi(\boldsymbol{k}_1)\Pi(\boldsymbol{k}_2)\Pi(\boldsymbol{k}_3)} \\ \quad\times\left[1-\dfrac{1}{3}\dfrac{1}{M_3(\boldsymbol{k}_1,\boldsymbol{k}_2,\boldsymbol{k}_3)}\left\{\dfrac{M_2(\boldsymbol{k}_1,\boldsymbol{k}_2+\boldsymbol{k}_3)M_2(\boldsymbol{k}_2,\boldsymbol{k}_3)}{\Pi(\boldsymbol{k}_{23})}+\text{perm.}\right\}\right] & ;\ (a,b,c,d)=(2,1,1,1), \\ 0 & ;\ \text{otherwise}. \end{cases} \tag{3.13}$$

Again this term is absent in GR. The vertex function $\sigma_{abcd}(\boldsymbol{k}_1,\boldsymbol{k}_2,\boldsymbol{k}_3;\tau)$ defined above is invariant under the permutation of $b \leftrightarrow c \leftrightarrow d$ or $\boldsymbol{k}_1 \leftrightarrow \boldsymbol{k}_2 \leftrightarrow \boldsymbol{k}_3$.

IV. EVOLUTION EQUATIONS FOR THE POWER SPECTRUM

In this paper, we are especially interested in the evolution of the matter power spectrum defined by

$$\Big\langle \Phi_a(\boldsymbol{k};\tau)\Phi_b(\boldsymbol{k}';\tau)\Big\rangle = (2\pi)^3\,\delta_{\rm D}(\boldsymbol{k}+\boldsymbol{k}')\,P_{ab}(|\boldsymbol{k}|;\tau). \tag{4.1}$$

Here the bracket $\langle\cdot\rangle$ stands for the ensemble average. Note that we obtain the three different power spectra: $P_{\delta\delta}$ from $(a,b)=(1,1)$, $-P_{\delta\theta}$ from $(a,b)=(1,2)$ and $(2,1)$, and $P_{\theta\theta}$ from $(a,b)=(2,2)$.

Let us consider how to compute the power spectrum. In the standard perturbation theory (SPT), we first solve Eq.(3.8) by expanding the quantity Φ_a as $\Phi_a = \Phi_a^{(1)} + \Phi_a^{(2)} + \cdots$. Substituting the perturbative solutions into the definition (4.1), we obtain the weakly non-linear corrections to the power spectrum. This treatment is straightforward, but it is not suited for numerical calculations. Furthermore, successive higher-order corrections generally converge poorly and SPT will be soon inapplicable at the late-time stage of the non-linear evolution. Here in order to deal with modified gravity models, in which analytical calculation is intractable in many cases, we take an alternative approach. Our approach is based on the closure approximation proposed by Ref. [37], by which the evolution of the power spectrum is obtained numerically by solving a closed set of evolution equations.

Provided the basic equation (3.8), evolution equations for the power spectrum can be derived by truncating an infinite chain of the moment equations with a help of perturvative calculations called the closure approximation. We skip the details of the derivation and present the final results. Readers who are interested in the derivation can refer to Ref. [37]. The resultant evolution equations are the coupled equations characterized by the three statistical quantities including the power spectrum. We define

$$\begin{aligned}
&\Big\langle \Phi_a(\boldsymbol{k};\tau)\Phi_b(\boldsymbol{k}';\tau')\Big\rangle = (2\pi)^3\,\delta_{\rm D}(\boldsymbol{k}+\boldsymbol{k}')\,R_{ab}(|\boldsymbol{k}|;\tau,\tau') \quad ; \qquad \tau>\tau',\\
&\left\langle \frac{\delta\Phi_a(\boldsymbol{k};\tau)}{\delta\Phi_b(\boldsymbol{k}';\tau')}\right\rangle = \delta_{\rm D}(\boldsymbol{k}-\boldsymbol{k}')\,G_{ab}(\boldsymbol{k}|\tau,\tau') \quad ; \qquad \tau\geq\tau'.
\end{aligned} \tag{4.2}$$

The quantities R_{ab} and G_{ab} denote the cross spectra between different times and the non-linear propagator, respectively. Note that $R_{ab}\neq R_{ba}$, in general. Then, the closure equations become

$$\begin{aligned}
\widehat{\Sigma}_{abcd}(k;\tau)\,P_{cd}(k;\tau) \;=\;& \int\frac{d^3\boldsymbol{q}}{(2\pi)^3}\Big[\gamma_{apq}(\boldsymbol{q},\boldsymbol{k}-\boldsymbol{q};\tau)\,F_{bpq}(-\boldsymbol{k},\boldsymbol{q},\boldsymbol{k}-\boldsymbol{q};\tau)+\gamma_{bpq}(\boldsymbol{q},-\boldsymbol{k}-\boldsymbol{q};\tau)\,F_{apq}(\boldsymbol{k},\boldsymbol{q},-\boldsymbol{k}-\boldsymbol{q};\tau)\Big]\\
&+3\int\frac{d^3\boldsymbol{q}}{(2\pi)^3}\Big[\sigma_{apqr}(\boldsymbol{q},-\boldsymbol{q},\boldsymbol{k};\tau)P_{pq}(q;\tau)P_{rb}(k;\tau)+\sigma_{bpqr}(\boldsymbol{q},-\boldsymbol{q},-\boldsymbol{k};\tau)\,P_{pq}(q;\tau)P_{ra}(k;\tau)\Big],
\end{aligned} \tag{4.3}$$

$$\begin{aligned}
\widehat{\Lambda}_{ab}(k;\tau)\,R_{bc}(k;\tau,\tau') \;=\;& \int\frac{d^3\boldsymbol{q}}{(2\pi)^3}\gamma_{apq}(\boldsymbol{q},\boldsymbol{k}-\boldsymbol{q};\tau)\,K_{cpq}(-\boldsymbol{k},\boldsymbol{q},\boldsymbol{k}-\boldsymbol{q};\tau,\tau')\\
&+3\int\frac{d^3\boldsymbol{q}}{(2\pi)^3}\sigma_{apqr}(\boldsymbol{q},-\boldsymbol{q},\boldsymbol{k};\tau)P_{pq}(q;\tau)R_{rc}(k;\tau,\tau'),
\end{aligned} \tag{4.4}$$

$$\begin{aligned}
\widehat{\Lambda}_{ab}(k;\tau)\,G_{bc}(k|\tau,\tau') \;=\;& 4\int_{\tau'}^{\tau}d\tau''\int\frac{d^3\boldsymbol{q}}{(2\pi)^3}\gamma_{apq}(\boldsymbol{q},\boldsymbol{k}-\boldsymbol{q};\tau)\,\gamma_{lrs}(-\boldsymbol{q},\boldsymbol{k};\tau'')G_{ql}(|\boldsymbol{k}-\boldsymbol{q}||\tau,\tau'')R_{pr}(q;\tau,\tau'')G_{sc}(k|\tau'',\tau'),\\
&+3\int\frac{d^3\boldsymbol{q}}{(2\pi)^3}\sigma_{apqr}(\boldsymbol{q},-\boldsymbol{q},\boldsymbol{k};\tau)P_{pq}(q;\tau)G_{rc}(k|\tau,\tau'),
\end{aligned} \tag{4.5}$$

where the operators $\widehat{\Sigma}_{abcd}$ and $\widehat{\Lambda}_{ab}$ are defined as

$$\widehat{\Sigma}_{abcd}(k;\tau)=\delta_{ac}\delta_{bd}\frac{\partial}{\partial\tau}+\delta_{ac}\Omega_{bd}(k;\tau)+\delta_{bd}\Omega_{ac}(k;\tau),\quad \widehat{\Lambda}_{ab}(k;\tau)=\delta_{ab}\frac{\partial}{\partial\tau}+\Omega_{ab}(k;\tau), \tag{4.6}$$

The explicit expressions for the kernels F_{apq} and K_{cpq} are summarized as

$$F_{apq}(\boldsymbol{k},\boldsymbol{p},\boldsymbol{q};\tau) = 2\int_{\tau_0}^{\tau} d\tau'' \Big[2\, G_{ql}(q|\tau,\tau'')\,\gamma_{lrs}(\boldsymbol{k},\boldsymbol{p};\tau'')\, R_{ar}(k;\tau,\tau'')R_{ps}(p;\tau,\tau'') + G_{al}(k|\tau,\tau'')\,\gamma_{lrs}(\boldsymbol{p},\boldsymbol{q};\tau'')\, R_{pr}(p;\tau,\tau'')\, R_{qs}(q;\tau,\tau'') \Big], \tag{4.7}$$

$$\begin{aligned} K_{cpq}(\boldsymbol{k}',\boldsymbol{p},\boldsymbol{q};\tau,\tau') &= 4\int_{\tau_0}^{\tau} d\tau''\, G_{ql}(q|\tau,\tau'')\,\gamma_{lrs}(\boldsymbol{k}',\boldsymbol{p};\tau'')\, R_{ps}(p;\tau,\tau'') \\ &\quad\times \Big\{ R_{cr}(k';\tau',\tau'')\Theta(\tau'-\tau'') + R_{rc}(k';\tau'',\tau')\Theta(\tau''-\tau') \Big\} \\ &\quad + 2\int_{\tau_0}^{\tau'} d\tau''\, G_{cl}(k'|\tau',\tau'')\,\gamma_{lrs}(\boldsymbol{p},\boldsymbol{q};\tau'')\, R_{pr}(p;\tau,\tau'')\, R_{qs}(q;\tau,\tau''). \end{aligned} \tag{4.8}$$

The closure equations (4.3)–(4.5) are the integro-differential equations involving several non-linear terms, in which the information of the higher-order corrections in SPT is encoded. Thus, replacing all statistical quantities in these non-linear terms with linear-order ones, the solutions of the closure equations automatically reproduce the leading-order results of SPT, so called one-loop power spectra. Further, a fully non-linear treatment of the closure equations provides a non-perturbative description of the power spectra, and has an ability to predict the matter power spectra accurately beyond one-loop SPT. Strictly speaking, the non-linear terms in the right-hand side of Eqs. (4.3)–(4.5) have only an information of the one-loop corrections. However, it has been shown in Ref. [37] that the present formulation are equivalent to the one-loop level of renormalized perturbation theory by Crocce and Scoccimarro [39] and 2PI effective action method by Valageas [40], and even the leading-order approximation still contain some non-perturbative effects. The application of the closure approximation, together with the detailed comparison with N-body simulations, is presented in Refs. [38, 51]. Also, comprehensive discussion on the differences between several (semi-)analytic prescriptions for computing non-linear power spectrum, including the closure approximation, is found in Ref. [52].

In this paper, we mainly use the closure equations for the purpose of computing the one-loop power spectra. The results for the fully non-linear treatment of the closure equations will be presented elsewhere. The numerical scheme to solve the closure equations is basically the same as the one described in Ref. [53]. In Appendix A, we briefly review the numerical scheme and summarize several modifications.

Before closing this section, we note here that the resultant equations (4.3)–(4.5) contain the additional non-linear terms originating from the modification of the Poisson equation (see Eq.(3.4)). In particular, the terms containing the higher-order vertex function σ_{abcd} can be effectively absorbed into the matrix Ω_{ab}. Since the non-vanishing contribution of the higher-order vertex function only comes from σ_{2111}, this means that the effective Newton constant $G_{\rm eff}$ defined by (3.10) is renormalised as $G_{\rm eff} \to G_{\rm eff} + \delta G_{\rm eff}$, with $\delta G_{\rm eff}$ given by

$$\delta G_{\rm eff} = \frac{3H^2}{4\pi\,\rho_m}\int \frac{d^3\boldsymbol{q}}{(2\pi)^3}\,\sigma_{2111}(\boldsymbol{q},-\boldsymbol{q},\boldsymbol{k};\tau)\,P_{11}(q;\tau). \tag{4.9}$$

This is a clear manifestation of the mechanism to recover GR on small scales through the renormalisation of the Newton constant and, due to this mechanism, the growth rate of structure formation is altered on non-linear scales.

V. APPLICATIONS

In this section, based on the formulations presented in Sec. II and III, we compute the one-loop power spectrum in specific models of modified gravity theory. The models considered here are DGP braneworld models and $f(R)$ gravity models, which we will in turn discuss in Sec. V A and V B, respectively.

A. DGP models

In this subsection, we consider DGP braneworld models [45] as a representative example of modified gravity models in the context of higher-dimensional cosmology. In this model, it is possible to derive the quasi non-linear power spectrum analytically as is discussed in details in Appendix B. This provides us a check of our numerical code explained in the previous section and Appendix A.

1. DGP models

In DGP models, we are supposed to be living in a 4D brane in a 5D spacetime. The model is described by the action given by

$$S = \frac{1}{4\kappa^2 r_c}\int d^4x\sqrt{-g_5}R_5 + \frac{1}{2\kappa^2}\int d^4x\sqrt{-g}(R + L_{\rm m}), \tag{5.1}$$

where $\kappa^2 = 8\pi G$, R_5 is the Ricci scalar in 5D and $L_{\rm m}$ stands for the matter Lagrangian confined on a brane. The cross over scale r_c is the parameter in this model which is a ratio between the 5D Newton constant and the 4D Newton constant. The modified Friedman equation is given by

$$\epsilon\frac{H}{r_c} = H^2 - \frac{\kappa^2}{3}\rho, \tag{5.2}$$

where $\epsilon = \pm 1$ represents two distinct branches of the solutions [54]. From this modified Friedman equation, we find that the cross-over scale r_c must be fine-tuned to be the present-day horizon scales in order to modify gravity only at late times. The solution with $\epsilon = +1$ is known as the self-accelerating branch because even without the cosmological constant, the expansion of the Universe is accelerating as the Hubble parameter is constant, $H = 1/r_c$. On the other hand $\epsilon = -1$ corresponds to the normal branch. In this branch, we need a cosmological constant to realize the cosmic acceleration. However, due to the modified gravity effects, the Universe behaves as if it were filled with the Phantom dark energy with the equation of state w smaller than -1 [55, 56]. It is known that the self-accelerating solution is plagued by the ghost instabilities (see [57] for a review). Also it gives a poor fit to the observations such as supernovae and cosmic microwave background anisotropies [58, 59, 60].

However, this model is the simplest modified gravity model where the mechanism to recover of GR on small scales is naturally encoded and it can be used to get insights into the effect of this mechanism on the non-linear power spectrum. Also in this model, it is possible to derive analytic expressions for the quasi non-linear power spectrum. Thus it offers a check of our numerical code to solve the evolution equations for the power spectrum.

In this model, gravity becomes 5D on large scales larger than r_c. On small scales, gravity becomes 4D but it is not described by GR. The quasi-static perturbations are described by the BD theory where the BD parameter is given by [61]

$$\omega_{\rm BD}(\tau) = \frac{3}{2}\Big(\beta(\tau) - 1\Big), \quad \beta(\tau) = 1 - 2\epsilon H r_c\left(1 + \frac{\dot{H}}{3H^2}\right), \tag{5.3}$$

where $\dot{H}$ is the cosmic time derivative of the Hubble parameter H. Note that the BD parameter depends on time in this model. The BD scalar is massless $M_1 = 0$. However, it acquires a large second order interaction given by [48]

$$\mathcal{I}(\varphi) = \frac{r_c^2}{a^4}\Big[(\nabla^2\varphi)^2 - (\nabla_i\nabla_j\varphi)^2\Big]. \tag{5.4}$$

Note that r_c is tuned to be the present-day horizon scale. Thus this second order term has a large effect. The higher order terms than the second order are suppressed by the additional powers of the 4D Planck scale and, in the Newtonian limit, we can safely ignore them. Therefore, in this model, we have

$$M_1 = 0, \quad M_2(\boldsymbol{k}_1, \boldsymbol{k}_2) = 2\frac{r_c^2}{a^4}\Big[k_1^2k_2^2 - (\boldsymbol{k}_1\cdot\boldsymbol{k}_2)^2\Big], \quad M_3 = 0, \tag{5.5}$$

$$\Pi(k,\tau) = \beta(\tau)\frac{k^2}{a^2}. \tag{5.6}$$

In this paper, we use the best-fit cosmological parameters for the flat self-accelerating universe: $\Omega_m = 0.258, \Omega_b = 0.0544, h = 0.66, n_s = 0.998$ [60]. For the normal branch, we add the cosmological constant $\Omega_\Lambda = 1.5$.

It has been suggested that the idea of the self-acceleration could be extended to more general models and in these models one could avoid the ghost instabilities [62]. Although the covariant theory that realizes this idea is not known yet but our formalism can be applied to calculate the non-linear power spectrum in these models. In fact, in our formalism, this new model corresponds to add a new term M_3 (and also a constant term in $\mathcal{I}$). We will leave it as a future work to study these extensions.

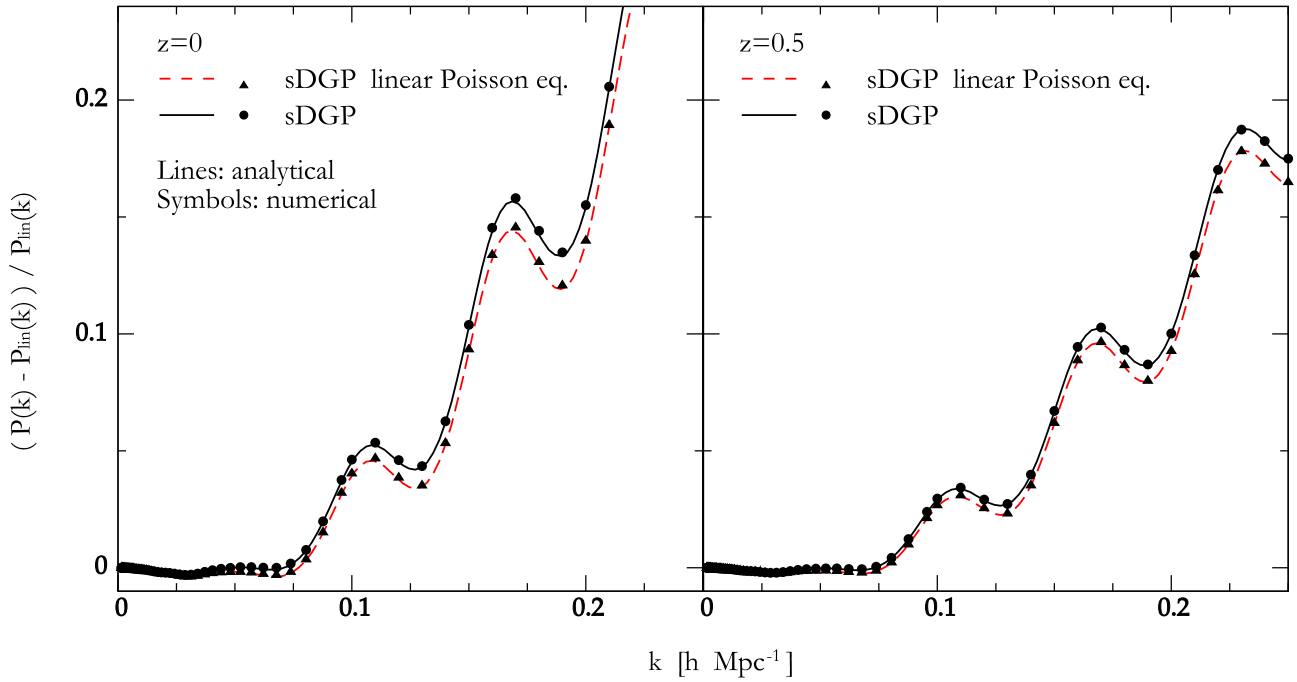

FIG. 1: Fractional change in the non-linear power spectrum relative to the linear power spectrum in the self-accelerating branch of DGP. The solid (black) line is the analytic solutions and the circles are numerical solutions obtained by solving the closure equation. The dashed (red) line shows the analytic solutions obtained by neglecting the non-linear interaction terms $\mathcal{I}$. The triangles represent the numerical solutions in this case. We used the best fit cosmological parameters for the flat universe $\Omega_m = 0.258, \Omega_b = 0.0544, h = 0.66, n_s = 0.998$.

2. *Quasi non-linear power spectra*

Fig. 1 shows a fractional change in the non-linear power spectrum for density perturbations relative to the linear power spectrum in the self-accelerating branch. In order to see the effect of the non-linear interaction term $\mathcal{I}$, we also plotted the non-linear power spectrum obtained from the linear Poisson equation by neglecting the interaction term $\mathcal{I}$. Although the differences between the two spectra are small in the quasi non-linear regime, we can see that the non-linear interaction term $\mathcal{I}$ enhances the non-linear power spectrum. This is natural because in the self-accelerating branch, the linear growth rate is suppressed compared to the GR model that follows the same expansion history. The suppression is due to the negative BD parameter $\omega_{\rm BD} < 0$ in this model, which makes the Newton constant smaller than GR. This is closely related to the fact that the BD scalar becomes a ghost. Classically, the ghost mediates a repulsive force and suppresses the gravitational collapse. The non-linear interaction makes the theory approach GR. Thus it effectively increases the Newton constant by screening the BD scalar. Then the power spectrum receives an enhancement compared with the case without the non-linear interaction.

Fig. 2 shows a fractional change in the non-linear power spectrum relative to the linear power spectrum in the normal branch. Again we showed the two cases with and without $\mathcal{I}$. In the normal branch, the linear growth rate is enhanced as the BD parameter is positive $\omega_{\rm BD} > 0$. Thus, the situation is completely opposite to the self-accelerating branch and the non-linear interaction suppresses the non-linear power spectrum in order to recover GR on small scales.

In both branches, it is possible to derive the solutions for the power spectrum analytically by solving the equation for perturbations (3.8) perturbatively

$$\Phi_a = \Phi_a^{(1)} + \Phi_a^{(2)} + \Phi_a^{(3)} + ... \tag{5.7}$$

The power spectrum is also expanded accordingly

$$P_{ab}(k;t) = P_{ab}^{(11)}(k;t) + P_{ab}^{(22)}(k;t) + P_{ab}^{(13)}(k;t) + ... \tag{5.8}$$

The detailed calculations are summarized in Appendix B. In Fig.1, we compare the results obtained by solving the closure equations numerically with those from the analytic solutions. In order to derive the analytic solutions,

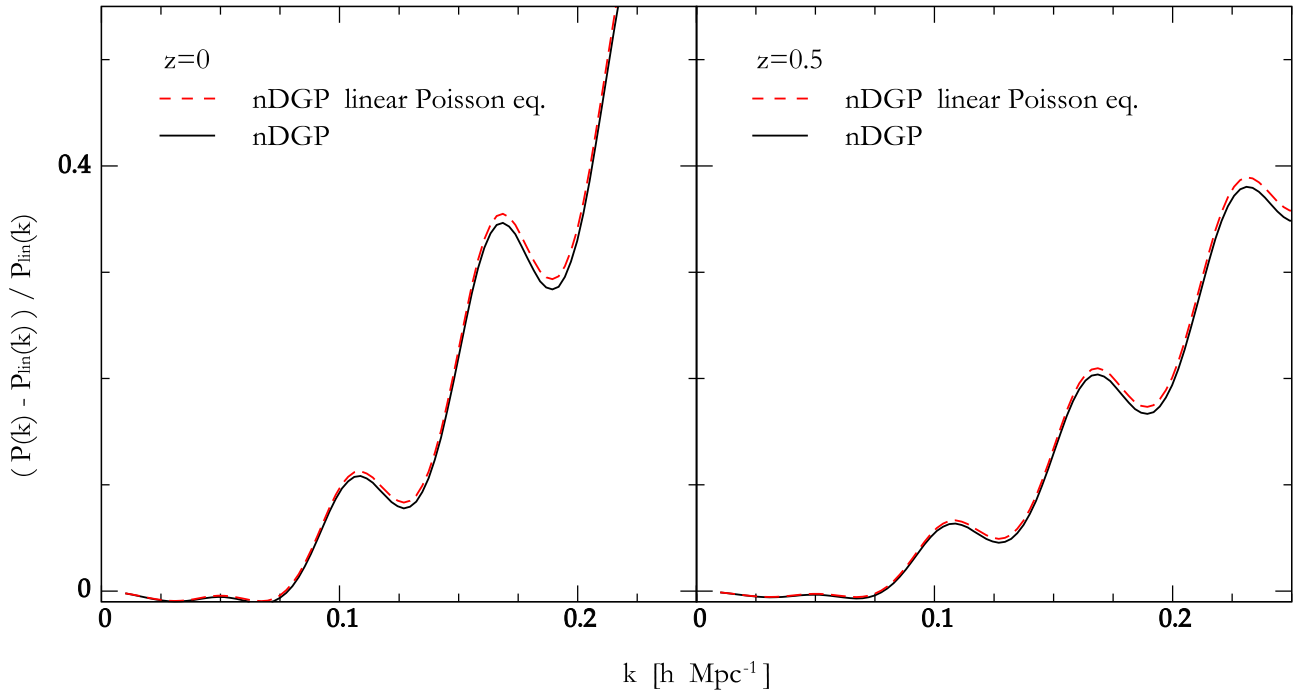

FIG. 2: The same in the normal branch as in Fig.1. We only show the analytic solutions. The numerical solutions agree with them very well. The cosmological parameters are the same as the self-accelerating universe but in addition there is a cosmological constant $\Omega_\Lambda = 1.5$.

we employed the Einstein-de Sitter (EdS) approximation. In the EdS approximation, all the non-linear growth rates appearing in the higher-order solutions are approximately determined by the linear growth rate $D_1(t)$. It is also possible to apply the EdS approximation in the numerical calculations [53] and we have checked that the EdS approximation changes the result only at sub percent level. The fact that the two results agree very well confirms the validity of our numerical code.

B. $f(R)$ gravity models

In this subsection, we derive the quasi non-linear power spectrum in $f(R)$ gravity model (see [27, 28] for reviews). In this model, N-body simulations have been performed [24, 25, 26] and we will check our numerical solutions against the full N-body simulations.

1. *$f(R)$ gravity models*

We consider another class of modified theory of gravity that generalizes the Einstein-Hilbert action to include an arbitrary function of the scalar curvature R:

$$S = \int d^4x\sqrt{-g}\left[\frac{R + f(R)}{2\kappa^2} + L_{\rm m}\right], \tag{5.9}$$

where $\kappa^2 = 8\pi\, G$ and $L_{\rm m}$ is the Lagrangian of the ordinary matter. This theory is equivalent to the BD theory with $\omega_{\rm BD} = 0$ but there is a non-trivial potential [63, 64]. This can be seen from the trace of modified Einstein equations:

$$3\Box f_R - R + f_R R - 2f = -\kappa^2\rho, \tag{5.10}$$

where $f_R = df/dR$ and $\Box$ is a Laplacian operator and we assumed matter dominated universe. We can identify f_R as the BD scalar field and its perturbations are defined as

$$\varphi = \delta f_R \equiv f_R - \overline{f}_R, \tag{5.11}$$

where the bar indicates that the quantity is evaluated on the cosmological background. In this paper, we assume $|\bar{f}_R| \ll 1$ and $|\bar{f}/\bar{R}| \ll 1$. These conditions are necessary to have the background close to ΛCDM cosmology. Then the BD scalar perturbations satisfy

$$3\frac{1}{a^2}\nabla^2\varphi = -\kappa^2\rho_m\delta + \delta R, \quad \delta R \equiv R(f_R) - R(\overline{f}_R). \tag{5.12}$$

This is nothing but the equation for the BD scalar perturbations with $\omega_{\rm BD} = 0$ and the potential gives the non-linear interaction term

$$\mathcal{I}(\varphi) = \delta R(\varphi). \tag{5.13}$$

Then we find

$$M_1 = \overline{R}_f(\tau) \equiv \frac{d\overline{R}(f_R)}{df_R}, \quad M_2 = \overline{R}_{ff}(\tau) \equiv \frac{d^2\overline{R}(f_R)}{df_R^2}, \quad M_3 = \overline{R}_{fff}(\tau) \equiv \frac{d^3\overline{R}(f_R)}{df_R^3},$$
$$\Pi(k,\tau) = \left(\frac{k}{a}\right)^2 + \frac{\overline{R}_f(\tau)}{3}.$$

We should note that in this model, the linear growth rate depends on the wave number. Due to this, the vertex functions are not the separable functions in terms of k and τ. This prevents us deriving the solutions analytically unlike the DGP case and we need to solve the closure equation directly.

In this paper, we consider the function $f(R)$ of the form

$$f(R) \propto \frac{R}{AR+1}, \tag{5.14}$$

where A is a constant with dimensions of length squared [33]. In the limit $R \to 0$, $f(R) \to 0$ and there is no cosmological constant. For high curvature $AR \gg 1$, $f(R)$ can be expanded as

$$f(R) \simeq -2\kappa^2\rho_\Lambda - f_{R0}\frac{\bar{R}_0^2}{R}, \tag{5.15}$$

where ρ_Λ is determined by A, $\bar{R}_0$ is the background curvature today and we defined f_{R0} as $f_{R0} = \bar{f}_R(R_0)$. As we mentioned before, we take $|f_{R0}| \ll 1$ and assume that the background expansion follows the Λ CDM history with the same ρ_Λ. The M_1 term determines the mass of the BD field $m_{\rm BD} = (M_1/3)^{1/2}$ as

$$m_{\rm BD}(\tau) \equiv \sqrt{\frac{\bar{R}_f}{3}} = \left(\frac{R_0}{6|\bar{f}_R|}\sqrt{\frac{f_{R0}}{\bar{f}_R}}\right)^{1/2}. \tag{5.16}$$

Above the Compton length $m_{\rm BD}^{-1}$, the BD scalar interaction decays exponentially and we recover GR. On small scales, we recover the BD theory with $\omega_{\rm BD} = 0$ if we neglect the higher order terms $M_i, (i > 1)$. From Eq. (3.11), the Newton constant is 4/3 times large than GR. Thus the linear power spectrum acquires a scale dependent enhancement on small scales. Of course, this model is excluded from local gravity constraints. The higher order terms $M_i (i > 1)$ are responsible for suppressing this modification of gravity on small scales via the chameleon mechanism and it makes possible to pass local gravity constraints. Thus we expect that the non-linear interaction terms $\mathcal{I}$ will suppress the non-linear power spectrum. In the following, when we mention the power spectrum with the chameleon mechanism, it means that we introduce the non-linear terms $\mathcal{I}$ derived from (5.14) which contains the mechanism to recover GR on small scales by screening the scalar mode. In this paper, we adopt the cosmological parameters given by $|f_{R0}| = 10^{-4}, n_s = 0.958, \Omega_m = 0.24, \Omega_b = 0.046, \Omega_\Lambda = 0.76, h = 0.73$.

In this model, the solar system constraints are satisfied but it has been pointed out that the chameleon mechanism does not work for strong gravity and neutron stars cannot exist [65, 66]. It was claimed that a fine-tuned higher curvature corrections to $f(R)$ is needed to cure the problem [67]. However, recently there appeared an objection against the absence of relativistic stars [68]. In this paper, we perturbatively take into account the chameleon mechanism in the cosmological background and the quasi non-linear power spectrum would be insensitive to the higher curvature corrections.

We should also mention that recently a couple of papers appear that study the second order perturbations and three point functions in $f(R)$ gravity models [69, 70].

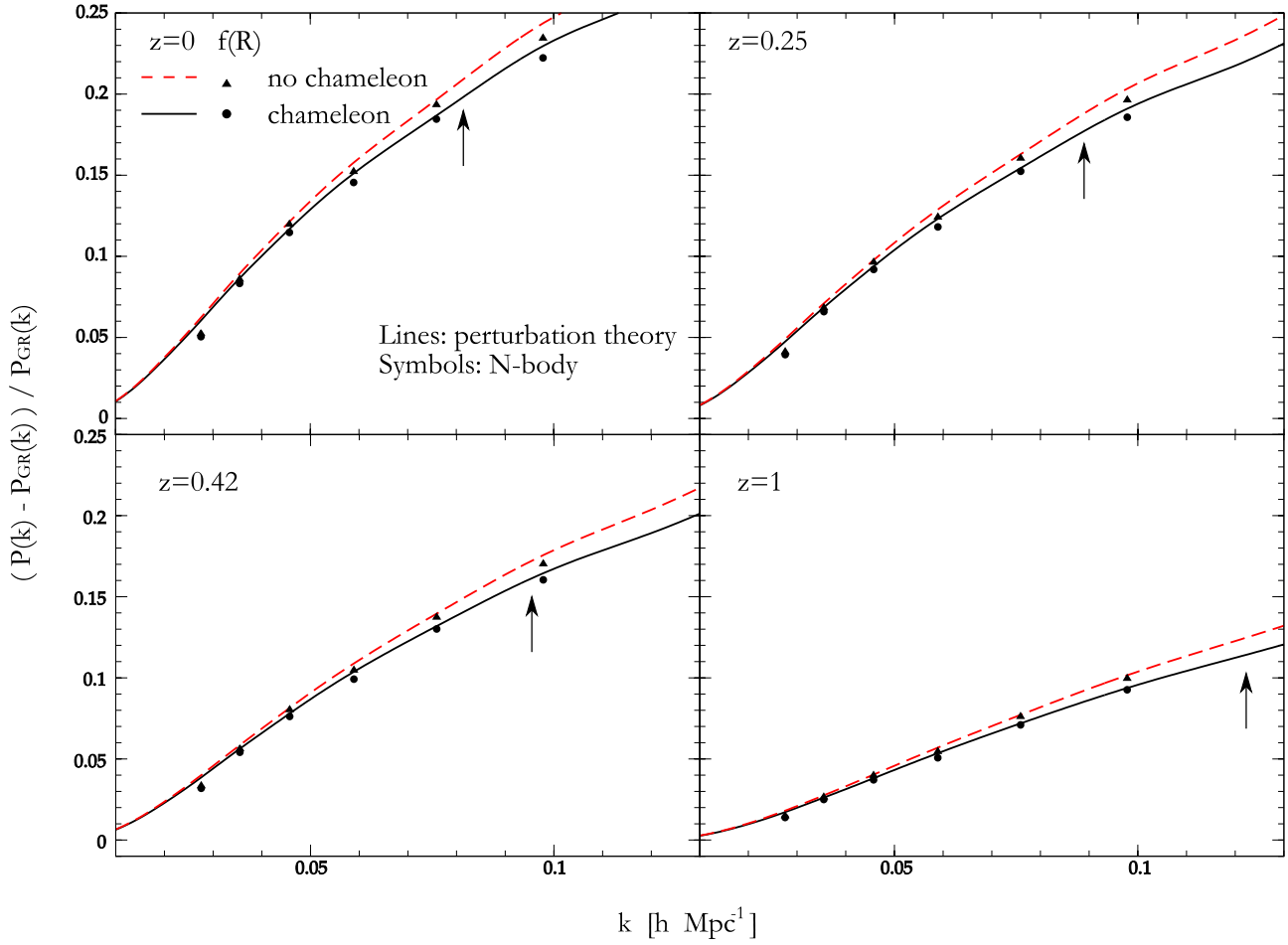

FIG. 3: Fractional change in the non-linear power spectrum in $f(R)$ gravity models relative to the GR models with the same expansion history. $P_{\rm GR}$ is the non-linear power spectrum in ΛCDM model with the same cosmological parameters. The solid (black) lines are the solutions in the perturbation theory obtained by solving the closure equation numerically. The circles show the results of N-body simulations. The dashed (red) line is the perturbation theory solutions obtained by neglecting the non-linear interaction terms $\mathcal{I}$. The triangles represent the corresponding N-body solutions. The arrow indicate the valid regime of the perturbation theory. The parameters are taken as $|f_{R0}| = 10^{-4}, n_s = 0.958, \Omega_m = 0.24, \Omega_b = 0.046, \Omega_\Lambda = 0.76, h = 0.73$.

2. *Quasi non-linear power spectra*

Fig. 3 shows a fractional change in the non-linear power spectrum in $f(R)$ gravity models relative to the GR model with the same expansion history, ΛCDM model. Note again that unlike the DGP case, the function Π is not a separable function of k and τ, and the analytical calculation is intractable. The solid line shows the case with the chameleon mechanism which includes the higher order terms M_2 and M_3. The dashed line shows the non-chameleon case where we neglected the higher order terms M_2 and M_3. As expected, the chameleon mechanism suppresses the non-linear power spectrum. The situation is similar to the normal branch DGP models.

We have also shown the results from N-body simulations in both cases [71]. The N-body simulations are performed under the quasi-static approximations. The form of $f(R)$ that is used in the simulations is the same as ours and we have checked that the basic equations that are used in their simulations are the same as our equations. They run the simulations with a box size $256h^{-1}$ Mpc and with 256^3 particles.The power spectrum starts to show systematic $> 10\%$ deviations from Smith et.al. fitting formula [72] for $k > 0.79h$ Mpc $^{-1}$. The arrow in the figure shows the expected validity range of the perturbation theory. We determine this validity regime of the perturbation theory by solving the equation

$$\frac{k^2}{6\pi^2}\int_0^k d^3q P_{\rm lin}(q,z) = 0.18, \tag{5.17}$$

for k, where $P_{\rm lin}$ is the linear power spectrum. This limit of k represents the range of the 1%-level accuracy, which has been empirically found by comparisons between the perturbation theory predictions and N-body simulations [38]. Of course, this condition was calibrated in simulations in GR and there is no guarantee that this condition can be applied to modified gravity models, but this limit gives an useful indication of the validity of the perturbations theory. In fact, we find that the agreement between the perturbations theory and N-body simulations in $f(R)$ theory is good within this validity regime of the perturbation theory.

VI. IMPLICATION FOR FULLY NON-LINEAR POWER SPECTRUM

We have developed the formalism to derive the quasi non-linear power spectrum. In this section, we study the Parametrized Post-Friedmann (PPF) framework for the non-linear power spectrum [5] in order to get insight into the fully non-linear power spectrum.

A. PPF formalism

Hu and Sawicki proposed a fitting formula for the non-linear power spectrum in modified gravity models [5]. The fitting formula based on the observation that the non-linear power spectrum should approach the one in the GR model that follows the same expansion history of the Universe due to the recovery of GR on small scales. They postulate that the fully non-linear power spectrum in a modified gravity model is given by the formula

$$P(k,z) = \frac{P_{\rm non-GR}(k,z) + c_{\rm nl}\Sigma^2(k,z)P_{\rm GR}(k,z)}{1+c_{\rm nl}\Sigma^2(k,z)}, \tag{6.1}$$

where z is a red-shift. Here $P_{\rm non-GR}(k,z)$ is the non-linear power spectrum which is obtained without the non-linear interactions that are responsible for the recovery of GR. This is equivalent to assume that gravity is modified down to the small scales in the same way as in the linear regime. $P_{\rm GR}(k,z)$ is the non-linear power spectrum obtained in the GR dark energy model that follows the same expansion history of the Universe as the modified gravity model. The function $\Sigma^2(k,z)$ determines the degree of non-linearity at a relevant wavenumber k. They propose to take $\Sigma^2(k) = k^3P_{\rm lin}(k,z)/2\pi^2$, where $P_{\rm lin}(k,z)$ is the linear power spectrum in the modified gravity model. Finally, $c_{\rm nl}$ is a parameter in this framework which controls the scale at which the theory approaches GR.

Once we obtain the quasi non-linear power spectrum, we can check whether the PPF framework works and determines $c_{\rm nl}$ in the quasi non-linear regime. In our formalism, $P_{\rm non-GR}(k,z)$ is obtained by neglecting the non-linear interaction $\mathcal{I}$. $P_{\rm GR}(k,z)$ can be obtained by taking $\omega_{\rm BD} \to \infty$ limit and also neglecting $\mathcal{I}$. We again consider two explicit examples.

B. DGP models

We first consider the self-accelerating branch solutions in DGP models. The extension to the normal branch solutions is straightforward though there is a subtlety in defining the equivalent dark energy model as the equation of state of dark energy becomes less than -1 and it diverges at some redshift [73]. Also an addition of curvature in the background is necessary to have large modified gravity effects [74]. We leave this for a future work. In the self-accelerating universe, we find that

$$\Sigma^2(k,z) = \frac{k^3}{2\pi^2}P_{\rm lin}(k,z), \tag{6.2}$$

as proposed by Hu and Sawicki [5] gives a nice fit to the results obtained in the perturbation theory. We find that by allowing the time dependence in $c_{\rm nl}$, it is possible to recover the solutions for the non-linear power spectrum very well within the validity regime of the perturbation theory determined by Eq. (5.17). At $z = 0$, $c_{\rm nl}$ is given by 0.3 and there is a slight redshift dependence (Fig. 4). For $0 \le z \le 1$, we find that $c_{\rm nl}$ can be approximately fitted as $c_{\rm nl} = 0.3(1+z)^{0.16}$.

Armed with this result, it is tempting to extend our analysis to the fully non-linear regime. In GR, there are several fitting formulae which provide the mapping between the linear power spectrum and non-linear power spectrum. It is impossible to apply these mapping formulae to modified gravity models as the mapping does not take into account the non-linear interaction terms $\mathcal{I}$ in the Poisson equation. If we apply the GR mapping formula to the linear power

spectrum, we would get the non-linear power spectrum without $\mathcal{I}$, that is, $P_{\rm non-GR}(k)$. In fact, there exists N-body simulations in DGP models performed by neglecting the non-linear interaction terms.

The mapping formulae should be valid in GR models, so we can also predict $P_{\rm GR}(k)$. Then using the PPF formalism (6.1), we can predict the non-linear power spectrum if $c_{\rm nl}$ is known. In the right panel of Fig. 4, we plotted a fractional change in the power spectrum in the DGP model relative to the GR model with the same expansion history. We used the fitting formula developed by Smith et.al. [72]. It should be noted that this fitting formula should be used with caution even in the simple case of dynamical dark energy [75] but given a lack of better fitting formula available at the moment, we used this formula as an example. If we could extrapolate the result in the quasi non-linear regime, we would have $c_{\rm nl} = 0.3$ at $z = 0$.

Recently, N-body simulations in DGP models have been done by Schmidt [76]. Fig.5 shows the comparison between the PPF prediction and N-body simulations. In the left panel of Fig. 5, the dashed line shows the power spectrum with the linear Poisson equation without $\mathcal{I}$. The corresponding N-body results are shown by triangles. Although Ref. [77] reported that the fitting formula works fine in this case, we find that the fitting formula by Smith.et.al. slightly overestimates the power spectrum [76]. The solid curve shows the full power spectrum including $\mathcal{I}$. Again the PPF formalism slightly overestimates the power spectrum. If we take the ratio between the two cases, the PPF formalism recovers N-body results up to $k = 0.5$Mpc h^{-1}. The validity regime of perturbation theory is below $k = 0.12$Mpc h^{-1}. Thus the PPF formalism using $c_{\rm nl}$ derived by the perturbation theory describes the effect of the Vainshtein mechanism on non-linear scales beyond the validity regime of the perturbation theory.

This observation suggests that an improvement of the PPF formalism can be made by getting a more accurate power spectrum without the Vainshtein mechanism because the PPF formalism describes the effect of the Vainshtein mechanism very well. In order to demonstrate this fact, we derive the power spectrum without the Vainsgtein mechanism $P_{\rm non-GR}$ by interpolating the N-body results (see the right panel of Fig. 5). Using this power spectrum as the power spectrum with the linear Poisson equation $P_{\rm non-GR}$ in the PPF formalism, we find that the full power spectrum can be very well described by the PPF formalism where $c_{\rm nl}$ is derived by the perturbation theory. We should emphasize that the ratio between the power spectra with and without the chameleon mechanism is not very sensitive to the power spectrum with the linear Poisson equation. This also indicates that the PPF formalism with $c_{\rm nl}$ determined by the perturbation theory describes the effect of the Vainshtein mechanism very well at least up to $k \sim 0.5h$Mpc^{-1}.

Above $k = 1$Mpch^{-1}, N-body simulations do not have enough resolutions. If we can extrapolate our results to this regime, we find that even at $k = 10$Mpch^{-1}, the difference between the power spectrum in DGP and that in the equivalent GR model remains at 7% level. This is crucial to distinguish between the two models using weak lensing as the signal to noise ratio is larger on smaller scales. Of course, we should emphasize that there is no guarantee that $c_{\rm nl}$ measured in the quasi non-linear regime is valid down to the fully non-linear scales and this should be tested by N-body simulations with higher resolutions.

C. $f(R)$ gravity models

Next, we consider $f(R)$ gravity models. As in the DGP model, we first check if we can reproduce the perturbation theory results by the PPF fitting. We find that the fitting is not very good if we adopt $\Sigma(k, z)$ as is proposed by Hu and Sawicki [5]. Instead, if we choose $\Sigma(k, z)$ as

$$\Sigma^2(k, z) = \left(\frac{k^3}{2\pi^2} P_{\rm lin}(k, z)\right)^{1/3}, \tag{6.3}$$

the solutions in the perturbation theory are fitted by the PPF formalism very well by allowing the redshift dependence in $c_{\rm nl}$. At $z = 0$, $c_{\rm nl} = 0.085$ gives an excellent fit to the power spectrum within the validity regime of the perturbation theory. For $0 \le z \le 1$, we find that $c_{\rm nl}$ can be approximately fitted as $c_{\rm nl} = 0.08(1 + z)^{1.05}$. In Fig. 6, we also show the prediction for the fractional difference between the power spectrum in $f(R)$ theory and that in ΛCDM model in fully non-linear regime for several $c_{\rm nl}$.

It is also possible to check our predictions against the N-body simulations done by Refs. [24, 25, 26]. Fig. 7 shows the comparison between the PPF prediction and N-body simulations. In the left panel, the dashed line corresponds to non-chameleon case with $c_{\rm nl} = 0$. The corresponding N-body results are shown by triangles. We again used the fitting formula by Smith et.al. to derive the non-linear power spectrum from the linear power spectrum. Compared with the N-body results, we find that, in this case, the formula by Smith et.al. slightly underestimates the power spectrum around $0.03h$Mpc$^{-1} < k < 0.5h$Mpc^{-1} and overestimates the power at $k > 0.5h$Mpc^{-1} though N-body simulations have large errors in this regime. The solid line shows the case with the chameleon mechanism. Again the PPF formalism underestimates the power spectrum in the same region as the non-chameleon case. If we

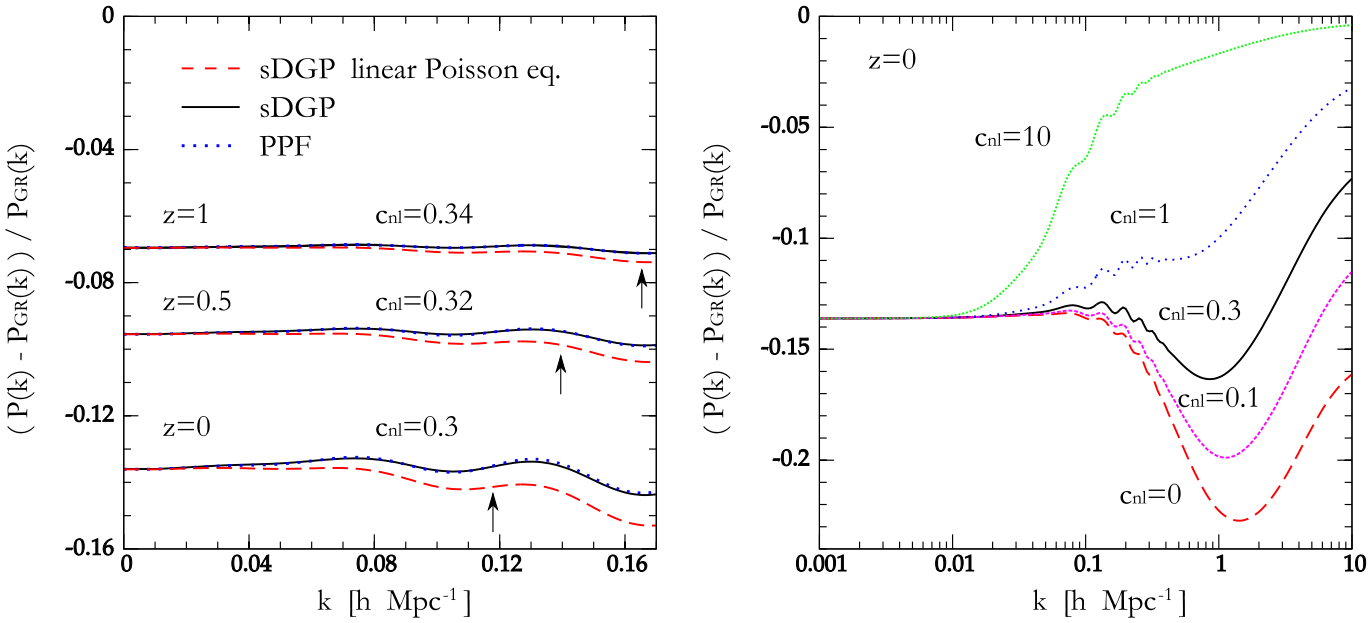

FIG. 4: A fractional change in the power spectrum in the DGP self-accelerating solution relative to the GR model which has the same expansion history as the DGP. The solid (black) line shows the perturbation theory solution and the dashed (red) line shows the perturbation theory solution without the non-linear interaction terms in the Poisson equation. The dotted (blue) line shows the PPF fitting. By allowing the redshift dependence of $c_{\rm nl}$, we can fit the power spectrum very well within the validity regime of the perturbation theory indicated by arrows. The right panel shows the results at $z = 0$ obtained from the fitting formula by Smith et.al. for $P_{\rm non-GR}$ and $P_{\rm GR}$. If $c_{\rm nl} = 0.3$ obtained by the perturbation theory is applicable, the solid (black) line is our prediction on non-linear scales. The cosmological parameters are the same as in Fig 1.

take the ratio between the non-chameleon case and chameleon case, the PPF formalism nicely recovers the N-body results up to $k \sim 0.5h{\rm Mpc}^{-1}$. Beyond that, N-body simulations have large errors. We should emphasize that the perturbation theory is valid only up to $k = 0.08h{\rm Mpc}^{-1}$ at $z = 0$. Thus the PPF formalism using $c_{\rm nl}$ derived by the perturbation theory describes the effect of the chameleon mechanism on non-linear scales beyond the validity regime of the perturbation theory.

As we have done in DGP models, we also derived the power spectrum without the chameleon mechanism $P_{\rm non-GR}$ by interpolating the N-body results (see the right panel of Fig. 7). Using this power spectrum as the non-chameleon power spectrum $P_{\rm non-GR}$ in the PPF formalism, we find that the power spectrum with the chameleon mechanism can be very well described by the PPF formalism where $c_{\rm nl}$ is derived by the perturbation theory. Again for larger k, N-body simulations also do not have enough resolutions and it is difficult to tell whether this extrapolation is good or not. More detailed study is needed to address the power spectrum at larger k, but the PPF formalism is likely to give a promising way to develop a fitting formula for the non-linear power spectrum in modified gravity models.

VII. CONCLUSIONS

In this paper, we developed a formalism to derive the quasi-nonlinear power spectrum for density perturbations in modified gravity models. We assume that the quasi-static perturbations under the horizon scale can be described by a BD theory with a time dependent BD parameter. The non-linear interaction terms are model-dependent so we parametrised these terms. Then we took into account the non-linear interaction terms perturbatively. The Poisson equation becomes a non-linear equation which relates the curvature perturbation to the density perturbations non-linearly. Then combining it to the continuity equation and Euler equation assuming the irrotationality of fluid quantities, we derived the evolution equations for the density perturbations and the velocity divergence in a compact form. The non-linearity of the Poisson equation introduces new vertex functions.

Then we derived the evolution equations for the power spectrum. The closure approximation was employed to derive a closed set of equations. In this paper, we further simplified the equations by replacing all the quantities in non-linear terms with linear-order ones. The resultant theory is equivalent to the standard perturbation theory where we solve the perturbations up to the third order. The advantage of using the closure equations is that we can directly integrate the evolution equations for the power spectrum numerically without using approximations to derive

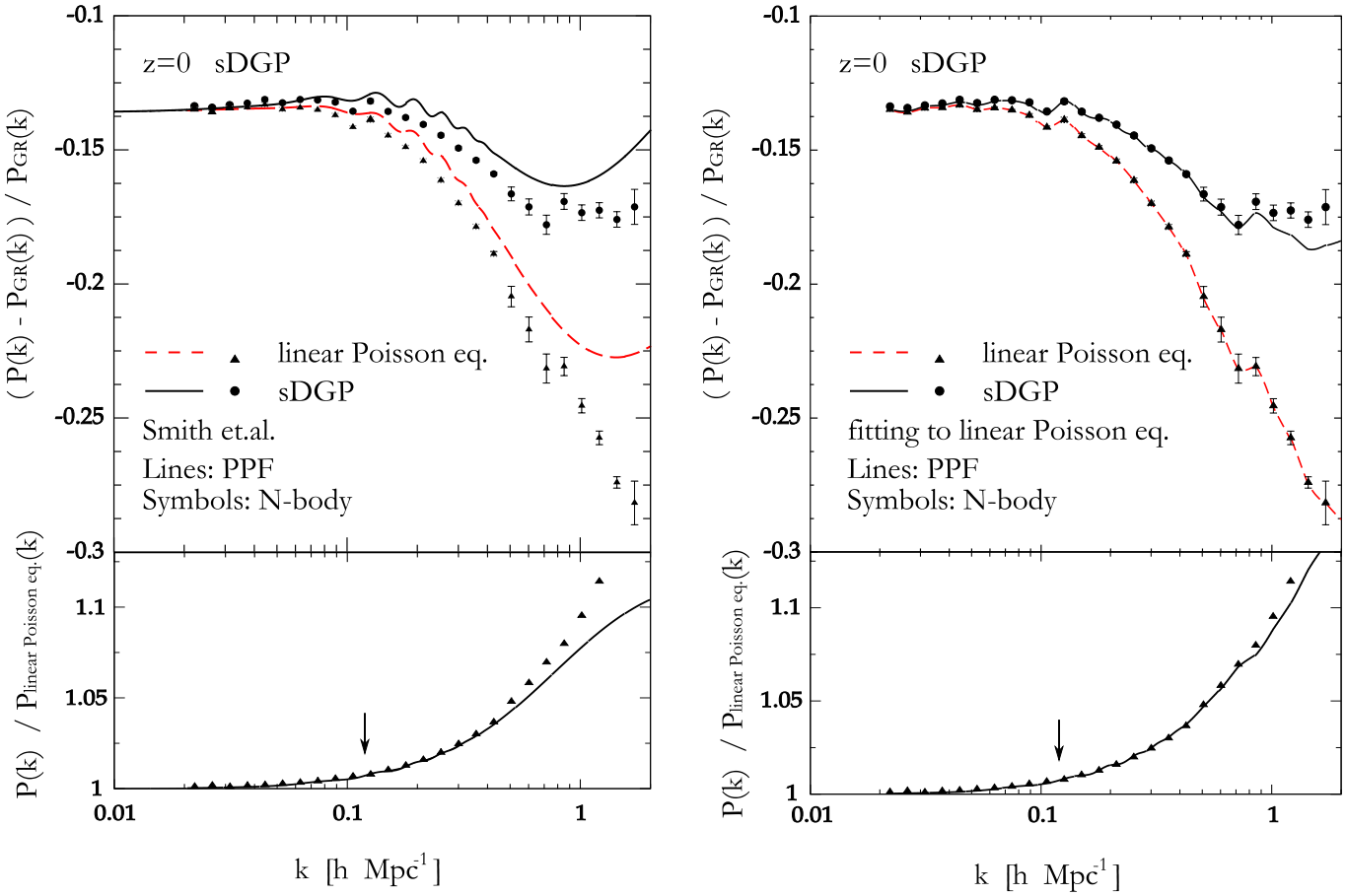

FIG. 5: Comparison between the PPF prediction and N-body simulations. In the left panel, Smith et.al. fitting formula is used to predict $P_{\rm non-GR}$ and $P_{\rm GR}$. We used $c_{\rm nl}$ determined by the perturbation theory $c_{\rm nl} = 0.3$ at $z = 0$. In the right panel, we fitted N-body results with the linear Poisson equation to derive $P_{\rm non-GR}$.

solutions for perturbations. The analysis of the full closure equations will be presented in a separate publication.

We solved the closure equations in DGP and $f(R)$ gravity models as examples. In the DGP model, the two branches of the solutions were considered. In the self-accelerating branch, the expansion of the Universe is accelerated without having the cosmological constant. In this branch, the BD parameter is negative and the linear growth rate is suppressed compared with the dark energy model that follows the same expansion history as the self-accelerating universe. We found that the non-linear interactions in the Poisson equation recover GR hence enhance the power spectrum by shielding the BD scalar interactions. On the other hand, in the normal branch solutions, where we need the cosmological constant to accelerate the expansion of the universe, the BD parameter is positive. Then the linear growth rate is enhanced compared to the corresponding dark energy model. In this case, the non-linearity of the Poisson equation suppresses the power spectrum. In DGP models, it is also possible to derive the semi-analytical solutions for the power spectrum by using the Einstein-de Sitter approximations for the growth rate. It was shown that the two methods give almost identical results. In $f(R)$ gravity models, it is impossible to derive semi-analytic solutions as the linear growth rate depends on scales. In this case, we compare our results with N-body simulations. Within the validity regime of the perturbation theory inferred from an empirical formula derived in GR simulations, our numerical solutions agree with N-body results very well. In $f(R)$ gravity models, the BD parameter is vanishing and gravity becomes strong below the Compton wavelength of the BD field and the linear growth rate acquires a scale dependent enhancement. Then the chameleon mechanism that recovers GR on small scales suppresses the power spectrum.

Recently, the parametrization of the non-linear power spectrum in modified gravity models was proposed within the framework of Parametrized Post Friedman (PPF) formalism. We checked whether the PPF formalism works or not explicitly using the solutions in the perturbation theory. In DGP models, we find that the PPF formalism works very well within the validity regime of the perturbation theory by allowing a time dependence in the PPF parameter $c_{\rm nl}$. The power spectrum without the mechanism to recover GR on small scales can be predicted by using a mapping

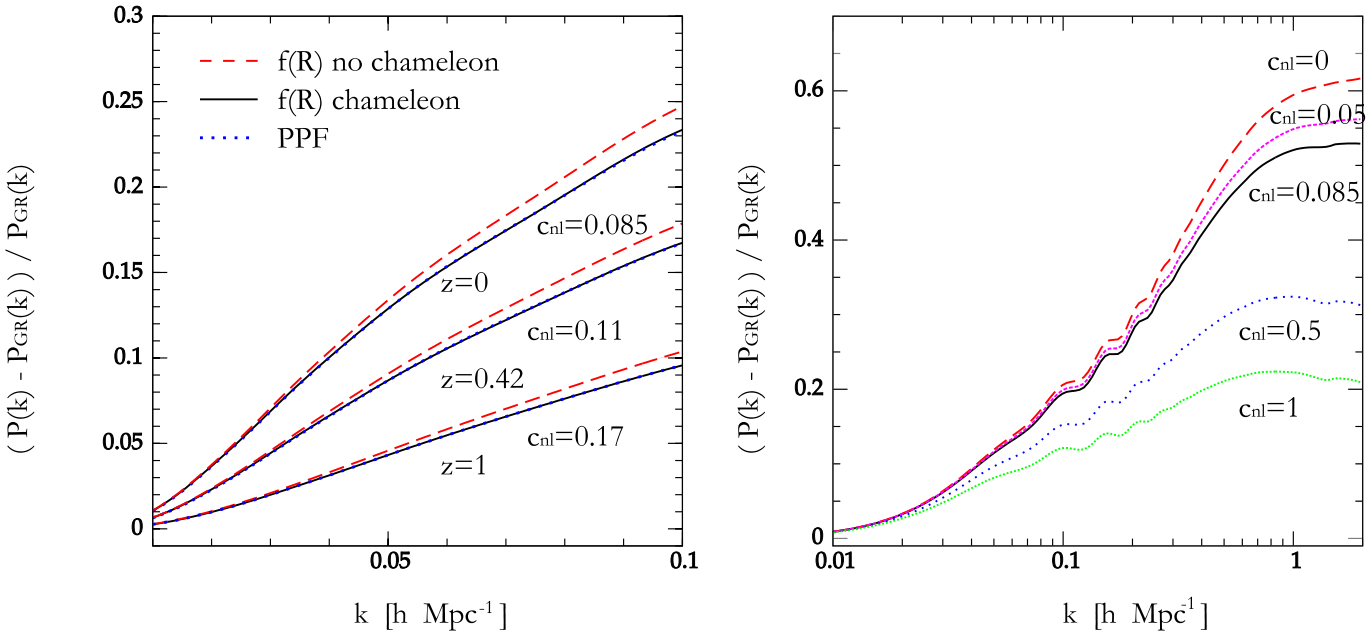

FIG. 6: The same as Fig. 4 in $f(R)$ gravity models

formula between the linear power spectrum and non-linear power spectrum derived in GR. We used a fitting formula obtained by Smith et.al which gives an accurate non-linear power spectrum in GR. Using the value of $c_{\rm nl}$ obtained in the perturbation theory, we predicted a fractional change in the non-linear power spectrum in DGP relative to the equivalent dark energy models. With the best fit cosmological parameters for SNe and CMB, there is a 14% change on linear scales and there is still a 7% change at $k = 10h{\rm Mpc}^{-1}$ at $z = 0$. Interestingly, the maximum change appears around $k = 1h{\rm Mpc}^{-1}$. We applied the same procedure to $f(R)$ gravity models. It was found that a slight modification was needed in the definition of $\Sigma(k, z)$ in the PPF formalism to reproduce the solutions in the perturbation theory. With this modification, we could reproduce the perturbation theory solutions very well again by allowing a time dependence in $c_{\rm nl}$. Then we predicted the fully non-linear power spectrum again using Smith et.al. fitting formula and the value of $c_{\rm nl}$ obtained in the perturbation theory.

We compared our PPF predictions with the N-body results in both cases. It was found that the PPF formalism reproduces the ratio between the power spectrum with and without the Vainshtein/chameleon mechanism very well beyond the validity regime of the perturbation theory. This indicates that the PPF formalism calibrated by the perturbation theory describes the effect of the Vainshtein/chameleon mechanism very well. On the other hand, Smith et.al. fitting formula does not predict the power spectrum without the Vainshtein/chameleon mechanism very accurately. In $f(R)$ gravity, this would be because the linear growth rate depends on scales. An improvement of the prediction can be made by obtaining the power spectrum without the Vainshtein/chameleon mechanism more accurately. In order to demonstrate this fact, we fitted the N-body results without the Vainshtein/chameleon mechanism and applied the PPF formalism to predict the power spectrum with the Vainsgtein/chameleon mechanism. In this way, it was shown that the PPF formalism calibrated by the perturbation theory reproduces the N-body results within the errors in N-body simulations. It should be pointed out that N-body simulations without the Veinshtein/chameleon mechanism is much easier to perform as the modified gravity effects reduce to the change of the Newton constant. On the other hand, if we need to include the Veinshtein/chameleon mechanism properly, it is necessary to solve the Klein-Gordon equation for the scalar field directly.

The understanding of the non-linear power spectrum is essential to distinguish between modified gravity models and dark energy models. Especially, weak lensing is sensitive to the clustering property on non-linear scales and all the predictions done by neglecting the mechanism to recover GR on small scales should be revisited. Our formalism based on the perturbation theory enables us to predict the quasi non-linear power spectrum very accurately. The PPF formalism calibrated by the perturbation theory gives an analytical way to predict non-linear power spectrum. Of course, we eventually need N-body simulations to check the predictions, but the PPF formalism will provide a way to develop a fitting formula for the non-linear power spectrum which is widely used to predict weak lensing signal in GR dark energy models. We tested our formalism in DGP and $f(R)$ gravity models but we should bear in mind that these models face serious difficulties. Our formalism is applicable to a wide variety of modified gravity models and it is ready to use once consistent models for modified gravity are developed.

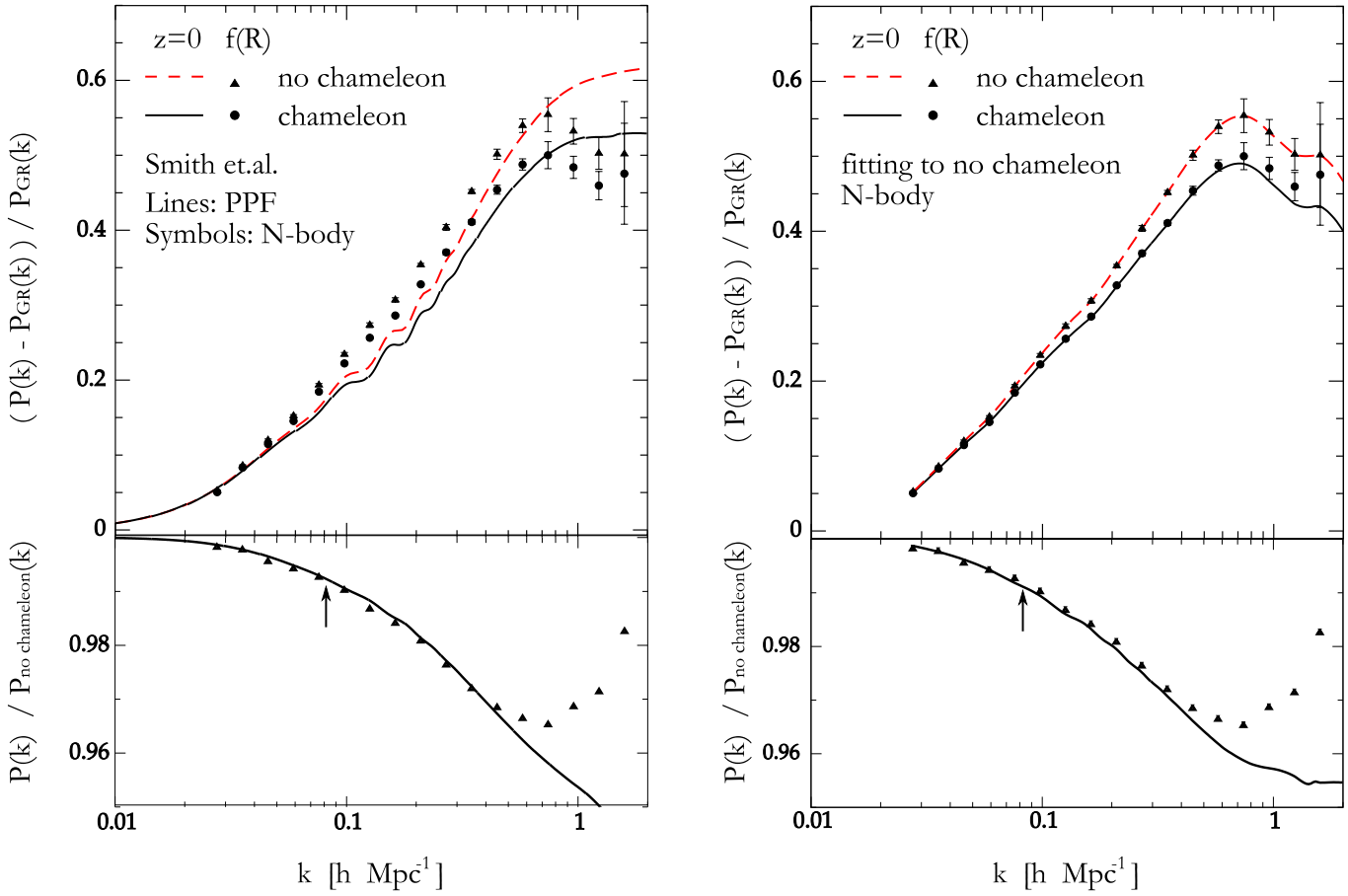

FIG. 7: Comparison between the PPF prediction and N-body simulations in $f(R)$ gravity models. In the left panel, Smith et.al. fitting formula is used to predict $P_{\rm non-GR}$ and $P_{\rm GR}$. We used $c_{\rm nl}$ determined by the perturbation theory $c_{\rm nl} = 0.085$ at $z = 0$. In the right panel, we fitted N-body results without the chameleon mechanism to derive $P_{\rm non-GR}$.

Acknowledgments

We would like to thank Wayne Hu and Fabian Schmidt for providing us their N-body data and for useful discussions. KK is supported by ERC, RCUK and STFC. AT is supported by a Grant-in-Aid for Scientific Research from the Japan Society for the Promotion of Science (JSPS) (No. 21740168). This work was supported in part by Grant-in-Aid for Scientific Research on Priority Areas No. 467 "Probing the Dark Energy through an Extremely Wide and Deep Survey with Subaru Telescope", and JSPS Core-to-Core Program "International Research Network for Dark Energy".

APPENDIX A: NUMERICAL ALGORITHM

In this paper, we follow the numerical scheme presented in [53] to solve the closure equations derived in [37]. The basic procedure to solve Eqs. (4.3)–(4.5) is the same as the one summarised in Sec.III in [53]. In what follows, we focus on the modifications that are necessary to apply it to modified gravity models.

In [53], the integration over k has been performed before performing the time evolution thanks to the time-independent vertex functions which make the integrands separable functions in terms of time and k. In the present case, however, the integration over k has to be performed at each time step because the integrands are generally not separable due to the time-dependent vertex functions. Another different point from the previous work is the existence of the extra vertex function, σ_{2111}.

Here we extend our numerical scheme presented in [53] to include the above two new ingredients, the non-separable integrands and the extra vertex function. Firstly, we change the variable $\boldsymbol{k}'$ to $\boldsymbol{k} - \boldsymbol{k}'$ in the integrations over $\boldsymbol{k}'$ in

Eqs. (4.3)–(4.5), then we obtain a more symmetric form of the closure equations,

$$\hat{\Lambda}_{ab}G_{bc}(k|\tau,\tau') = \int_{\tau'}^{\tau} d\tau''\, M_{as}(k;\tau,\tau'')G_{sc}(k|\tau'',\tau') + S_{ar}(k;\tau)G_{rc}(k|\tau,\tau'), \tag{A1}$$

$$\begin{aligned}\hat{\Lambda}_{ab}R_{bc}(k;\tau,\tau') = &\int_{\tau_0}^{\tau} d\tau''\, M_{as}(k;\tau,\tau'')R_{\overline{sc}}(k;\tau'',\tau') + \int_{\tau_0}^{\tau'} d\tau''\, N_{a\ell}(k;\tau,\tau'')G_{c\ell}(k|\tau',\tau'') \\ &+ S_{ar}(k;\tau)R_{rc}(k;\tau,\tau'),\end{aligned} \tag{A2}$$

$$\begin{aligned}\hat{\Sigma}_{abcd}P_{cd}(k;\tau) = &\int_{\tau_0}^{\tau} d\tau''\, M_{as}(k;\tau,\tau'')R_{bs}(k;\tau,\tau'') + \int_{\tau_0}^{\tau} d\tau''\, N_{a\ell}(k;\tau,\tau'')G_{b\ell}(k|\tau,\tau'') \\ &+ S_{ar}(k;\tau)P_{rb}(k;\tau) + (a \leftrightarrow b),\end{aligned} \tag{A3}$$

where

$$M_{as}(k;\tau,\tau'') = 4\int \frac{d^3\boldsymbol{k}'}{(2\pi)^3}\gamma_{apq}(\boldsymbol{k}-\boldsymbol{k}',\boldsymbol{k}';\tau)\gamma_{\ell rs}(\boldsymbol{k}'-\boldsymbol{k},\boldsymbol{k};\tau'')G_{q\ell}(k'|\tau,\tau'')R_{pr}(|\boldsymbol{k}-\boldsymbol{k}'|;\tau,\tau''), \tag{A4}$$

$$N_{a\ell}(k;\tau,\tau'') = 2\int \frac{d^3\boldsymbol{k}'}{(2\pi)^3}\gamma_{apq}(\boldsymbol{k}-\boldsymbol{k}',\boldsymbol{k}';\tau)\gamma_{\ell rs}(\boldsymbol{k}-\boldsymbol{k}',\boldsymbol{k}';\tau'')R_{qs}(k';\tau,\tau'')R_{pr}(|\boldsymbol{k}-\boldsymbol{k}'|;\tau,\tau''), \tag{A5}$$

$$S_{ar}(k;\tau) = 3\int \frac{d^3\boldsymbol{k}'}{(2\pi)^3}\sigma_{apqr}(\boldsymbol{k}',-\boldsymbol{k}',\boldsymbol{k};\tau)P_{pq}(k';\tau), \tag{A6}$$

and

$$R_{\overline{sc}}(k;\tau'',\tau') \equiv \begin{cases} R_{sc}(k;\tau'',\tau'), & \tau'' > \tau', \\ R_{cs}(k;\tau',\tau''), & \tau'' < \tau'. \end{cases} \tag{A7}$$

The domain of the two-dimensional integrand (A4)–(A6) is determined by

$$k_{\rm min} \le |\boldsymbol{k}'|, |\boldsymbol{k}-\boldsymbol{k}'| \le k_{\rm max}, \tag{A8}$$

where we set $k_{\rm min} = 0.001h{\rm Mpc}^{-1}$ and $k_{\rm max} = 5h{\rm Mpc}^{-1}$ according to the convergence check performed in [53].

Next we introduce (X, Y, ϕ)-coordinates in the $\boldsymbol{k}'$ space. Suppose $\boldsymbol{k}$ is aligned to the k'_z axis in $\boldsymbol{k}'$ space. Then the elliptic coordinate is defined as

$$\boldsymbol{k}' = \frac{\boldsymbol{k}}{2} + \boldsymbol{q}, \quad \boldsymbol{q} = \begin{pmatrix} \sinh\zeta\sin\mu\cos\phi \\ \sinh\zeta\sin\mu\sin\phi \\ \cosh\zeta\cos\mu \end{pmatrix}. \tag{A9}$$

We introduce the XY-coordinate as

$$X = \cosh\zeta, \quad Y = \cos\mu, \tag{A10}$$

where $X \ge 1$ and $-1 \le Y \le 1$. In these coordinates, the domain (A8) is depicted as the shaded hexagonal shape in Fig.8. Then we perform the integration over the domain at each time step. Note that the integration over ϕ yields only a constant 2π. In the previous work, we used the trapezium rule for the integrations. Instead, in order to reduce the computational cost without loosing the numerical accuracy, we implement the two-dimensional Gaussian quadrature (GQ). The two-dimensional GQ is adopted to the circumscribed rectangle of the computational domain as shown in Fig. (8). The circumscribed rectangle is then transformed to a unit square domain, $(x, y) \in [-1:1] \times [-1:1]$. On the unit domain, the two-dimensional integration is approximated by

$$\int_{-1}^{1}\int_{-1}^{1} f(x,y)\,dxdy \approx \sum_{i,j}^{N_{GQ}} f(x_i,y_i)w_iw_j, \tag{A11}$$

where x_i and y_i are defined as zero points of the Legendre function, namely, $P_{N_{GQ}}(x_i) = 0$. The weight w_i is calculated by

$$w_i = \frac{2}{(1-x_i^2)[P'_{N_{GQ}}(x_i)]^2}, \tag{A12}$$

where the prime denotes derivative with respect to x (e.g., see [78]). The domain of the two-dimensional integrands (A8) is extended to the unit domain so that the integrands vanish on the extended region, and those on the grid (x_i, y_j) are computed by the cubic spline interpolation of the propagators and power spectra. Having checked the convergence of the numerical results, we fix the number of the grid points as $N_{GQ} = 31$.

For the time evolutions, we set the initial redshift as $z_0 = 400$, and the number of time steps as $N_z = 400$, which are chosen so that the final results become insensitive to these parameters at the order of 0.1%. The number of wave numbers for the propagator and power spectra is set to be $N_k = 100$, and the discrete points in the wave number space are taken so that they become dense around the baryon acoustic oscillation scale.

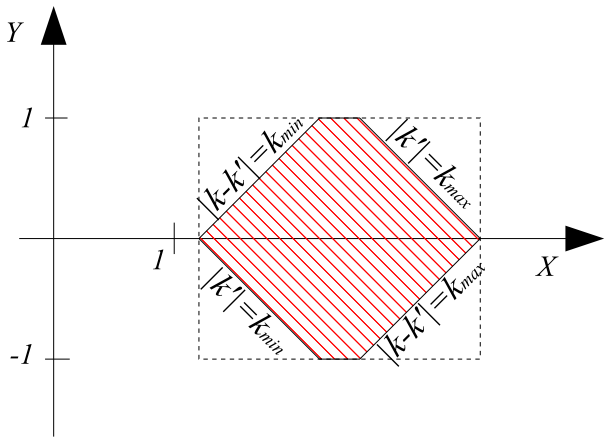

FIG. 8: The domain of the integrations in the integrations (A4)–(A6) in the (X, Y)-coordinate. The shadow region is defined by Eq. (A8) and, by definition, $-1 \leq Y \leq 1$. The circumscribed rectangle is the computational domain for the Gaussian quadrature.

APPENDIX B: PERTURBATION THEORY AND ONE-LOOP POWER SPECTRA IN DGP MODEL

In this appendix, we derive a set of perturbative solutions up to the third order in DGP models. Based on these solutions, we obtain the analytic expressions for the one-loop power spectra.

1. Solutions up to the third order

The solutions for δ and θ are perturbatively expanded as

$$\delta(\boldsymbol{k}) = \delta^{(1)}(\boldsymbol{k}) + \delta^{(2)}(\boldsymbol{k}) + \delta^{(3)}(\boldsymbol{k}) + \cdots, \quad \theta(\boldsymbol{k}) = \theta^{(1)}(\boldsymbol{k}) + \theta^{(2)}(\boldsymbol{k}) + \theta^{(3)}(\boldsymbol{k}) + \cdots. \tag{B1}$$

In order to obtain the solutions analytically, we use the Einstein-de Sitter (EdS) approximation (see sec.2.4.4 in [79] for a review). In the EdS approximation, all the non-linear growth rates appearing in the higher-order solutions are approximately determined by the linear growth rate $D_1(t)$. The explicit expressions for solutions at each order can be obtained analytically, and are summarized below.

1st-order solutions:

$$\delta^{(1)}(\boldsymbol{k}; t) = D_1(t)\delta_0(\boldsymbol{k}), \quad \theta^{(1)}(\boldsymbol{k}; t) = -(\dot{D}_1/H)\delta_0(\boldsymbol{k}), \tag{B2}$$

with D_1 being the linear growth rate. Here a dot denotes the derivative with respect to time and $\delta_0(\boldsymbol{k})$ denotes the primordial density perturbation defined at early matter dominated era. We assume $\delta_0(\boldsymbol{k})$ obeys Gaussian statistic. The evolution equation for D_1 is given by

$$\widehat{\mathcal{L}} D_1 = 0, \tag{B3}$$

where the linear operator $\widehat{\mathcal{L}}$ is given by

$$\widehat{\mathcal{L}} \equiv \frac{d^2}{dt^2} + 2H\frac{d}{dt} - \frac{\kappa}{2}\rho_m\left(1+\frac{1}{3\beta}\right). \tag{B4}$$

2nd-order solutions:

$$\delta^{(2)}(\boldsymbol{k};t) = \int \frac{d^3\boldsymbol{k}_1 d^3\boldsymbol{k}_2}{(2\pi)^3}\,\delta_{\rm D}(\boldsymbol{k}-\boldsymbol{k}_{12})\,\delta_0(\boldsymbol{k}_1)\delta_0(\boldsymbol{k}_2)\Big[D_1^2(t)\,F^{(2)}_{\rm sym}(\boldsymbol{k}_1,\boldsymbol{k}_2) + F_2(t)(1-\mu^2_{1,2})\Big], \tag{B5}$$

$$\theta^{(2)}(\boldsymbol{k};t) = \int \frac{d^3\boldsymbol{k}_1 d^3\boldsymbol{k}_2}{(2\pi)^3}\,\delta_{\rm D}(\boldsymbol{k}-\boldsymbol{k}_{12})\,\delta_0(\boldsymbol{k}_1)\delta_0(\boldsymbol{k}_2)\left[-(\dot{D}_1 D_1/H)\,G^{(2)}_{\rm sym}(\boldsymbol{k}_1,\boldsymbol{k}_2) - (\dot{F}_2/H)\,(1-\mu^2_{1,2})\right], \tag{B6}$$

where we define

$$\mu_{i,j} \equiv \frac{\boldsymbol{k}_i\cdot\boldsymbol{k}_j}{|\boldsymbol{k}_i|\,|\boldsymbol{k}_j|}. \tag{B7}$$

The symmetrized kernels of the integrals, $F^{(2)}_{\rm sym}$ and $G^{(2)}_{\rm sym}$, are respectively defined as

$$\begin{aligned} F^{(2)}_{\rm sym}(\boldsymbol{k}_1,\boldsymbol{k}_2) &= \frac{5}{14}\left\{\alpha(\boldsymbol{k}_1,\boldsymbol{k}_2)+\alpha(\boldsymbol{k}_2,\boldsymbol{k}_1)\right\} + \frac{1}{7}\beta(\boldsymbol{k}_1,\boldsymbol{k}_2),\\ G^{(2)}_{\rm sym}(\boldsymbol{k}_1,\boldsymbol{k}_2) &= \frac{3}{14}\left\{\alpha(\boldsymbol{k}_1,\boldsymbol{k}_2)+\alpha(\boldsymbol{k}_2,\boldsymbol{k}_1)\right\} + \frac{2}{7}\beta(\boldsymbol{k}_1,\boldsymbol{k}_2). \end{aligned}$$

Note that in addition to the linear growth rate D_1, the second-order solutions contain the new growth function F_2, which originates from the non-linearity of the Poisson equation. The evolution equation for F_2 is

$$\widehat{\mathcal{L}}F_2 = -\frac{r_{\rm c}^2}{6\beta^3}\left(\frac{\kappa\,\rho_m}{3}\right)^2 D_1^2. \tag{B8}$$

3rd-order solutions:

$$\begin{aligned} \delta^{(3)}(\boldsymbol{k};t) &= \int \frac{d^3\boldsymbol{k}_1 d^3\boldsymbol{k}_2 d^3\boldsymbol{k}_3}{(2\pi)^6}\,\delta_{\rm D}(\boldsymbol{k}-\boldsymbol{k}_{123})\,\delta_0(\boldsymbol{k}_1)\delta_0(\boldsymbol{k}_2)\delta_0(\boldsymbol{k}_3)\Big[D_1^3(t)\,F^{(3)}_{\rm sym}(\boldsymbol{k}_1,\boldsymbol{k}_2,\boldsymbol{k}_3) + C_3(t)\,C_{\rm sym}(\boldsymbol{k}_1,\boldsymbol{k}_2,\boldsymbol{k}_3)\\ &\quad + F_3(t)F_{\rm sym}(\boldsymbol{k}_1,\boldsymbol{k}_2,\boldsymbol{k}_3) + I_3(t)I_{\rm sym}(\boldsymbol{k}_1,\boldsymbol{k}_2,\boldsymbol{k}_3) + J_3(t)J_{\rm sym}(\boldsymbol{k}_1,\boldsymbol{k}_2,\boldsymbol{k}_3) + K_3(t)K_{\rm sym}(\boldsymbol{k}_1,\boldsymbol{k}_2,\boldsymbol{k}_3)\\ &\quad + L_3(t)L_{\rm sym}(\boldsymbol{k}_1,\boldsymbol{k}_2,\boldsymbol{k}_3)\Big], \end{aligned} \tag{B9}$$

$$\begin{aligned} \theta^{(3)}(\boldsymbol{k};t) &= \int \frac{d^3\boldsymbol{k}_1 d^3\boldsymbol{k}_2}{(2\pi)^6}\,\delta_{\rm D}(\boldsymbol{k}-\boldsymbol{k}_{123})\,\delta_0(\boldsymbol{k}_1)\delta_0(\boldsymbol{k}_2)\delta_0(\boldsymbol{k}_3)\Big[-(\dot{D}_1 D_1^2/H)\,G^{(3)}_{\rm sym}(\boldsymbol{k}_1,\boldsymbol{k}_2,\boldsymbol{k}_3) - (\dot{C}_3/H)\,C_{\rm sym}(\boldsymbol{k}_1,\boldsymbol{k}_2,\boldsymbol{k}_3)\\ &\quad - \{(\dot{F}_3 - \dot{D}_1 F_2)/H\}F_{\rm sym}(\boldsymbol{k}_1,\boldsymbol{k}_2,\boldsymbol{k}_3) - \{(\dot{I}_3 - D_1\dot{F}_2)/H\}I_3(t)I_{\rm sym}(\boldsymbol{k}_1,\boldsymbol{k}_2,\boldsymbol{k}_3)\\ &\quad - (\dot{J}_3/H)J_{\rm sym}(\boldsymbol{k}_1,\boldsymbol{k}_2,\boldsymbol{k}_3) - (\dot{K}_3/H)K_{\rm sym}(\boldsymbol{k}_1,\boldsymbol{k}_2,\boldsymbol{k}_3) - (\dot{L}_3/H)L_{\rm sym}(\boldsymbol{k}_1,\boldsymbol{k}_2,\boldsymbol{k}_3)\Big]. \end{aligned} \tag{B10}$$

The symmetrized kernels of integrals are

$$
\begin{aligned}
F^{(3)}_{\rm sym}(\boldsymbol{k}_1,\boldsymbol{k}_2,\boldsymbol{k}_3) &= \frac{1}{3}\left[\frac{2}{63}\beta(\boldsymbol{k}_1,\boldsymbol{k}_{23})\left\{\beta(\boldsymbol{k}_2,\boldsymbol{k}_3)+\frac{3}{4}\Big(\alpha(\boldsymbol{k}_2,\boldsymbol{k}_3)+\alpha(\boldsymbol{k}_3,\boldsymbol{k}_2)\Big)\right\}\right.\\
&\quad+\frac{1}{18}\alpha(\boldsymbol{k}_1,\boldsymbol{k}_{23})\left\{\beta(\boldsymbol{k}_2,\boldsymbol{k}_3)+\frac{5}{2}\Big(\alpha(\boldsymbol{k}_2,\boldsymbol{k}_3)+\alpha(\boldsymbol{k}_3,\boldsymbol{k}_2)\Big)\right\}\\
&\quad\left.+\frac{1}{9}\alpha(\boldsymbol{k}_{23},\boldsymbol{k}_1)\left\{\beta(\boldsymbol{k}_2,\boldsymbol{k}_3)+\frac{3}{4}\Big(\alpha(\boldsymbol{k}_2,\boldsymbol{k}_3)+\alpha(\boldsymbol{k}_3,\boldsymbol{k}_2)\Big)\right\}+\ \text{(cyclic perm.)}\right],\\
G^{(3)}_{\rm sym}(\boldsymbol{k}_1,\boldsymbol{k}_2,\boldsymbol{k}_3) &= \frac{1}{3}\left[\frac{2}{21}\beta(\boldsymbol{k}_1,\boldsymbol{k}_{23})\left\{\beta(\boldsymbol{k}_2,\boldsymbol{k}_3)+\frac{3}{4}\Big(\alpha(\boldsymbol{k}_2,\boldsymbol{k}_3)+\alpha(\boldsymbol{k}_3,\boldsymbol{k}_2)\Big)\right\}\right.\\
&\quad+\frac{1}{42}\alpha(\boldsymbol{k}_1,\boldsymbol{k}_{23})\left\{\beta(\boldsymbol{k}_2,\boldsymbol{k}_3)+\frac{5}{2}\Big(\alpha(\boldsymbol{k}_2,\boldsymbol{k}_3)+\alpha(\boldsymbol{k}_3,\boldsymbol{k}_2)\Big)\right\}\\
&\quad\left.+\frac{1}{21}\alpha(\boldsymbol{k}_{23},\boldsymbol{k}_1)\left\{\beta(\boldsymbol{k}_2,\boldsymbol{k}_3)+\frac{3}{4}\Big(\alpha(\boldsymbol{k}_2,\boldsymbol{k}_3)+\alpha(\boldsymbol{k}_3,\boldsymbol{k}_2)\Big)\right\}+\ \text{(cyclic perm.)}\right],\\
C_{\rm sym}(\boldsymbol{k}_1,\boldsymbol{k}_2,\boldsymbol{k}_3) &= \frac{1}{3}\left[\beta(\boldsymbol{k}_1,\boldsymbol{k}_{23})\,(1-\mu^2_{2,3})+\ \text{(cyclic perm.)}\right],\\
F_{\rm sym}(\boldsymbol{k}_1,\boldsymbol{k}_2,\boldsymbol{k}_3) &= \frac{1}{3}\left[\alpha(\boldsymbol{k}_1,\boldsymbol{k}_{23})\,(1-\mu^2_{2,3})+\ \text{(cyclic perm.)}\right],\\
I_{\rm sym}(\boldsymbol{k}_1,\boldsymbol{k}_2,\boldsymbol{k}_3) &= \frac{1}{3}\left[\alpha(\boldsymbol{k}_{23},\boldsymbol{k}_1)\,(1-\mu^2_{2,3})+\ \text{(cyclic perm.)}\right],\\
J_{\rm sym}(\boldsymbol{k}_1,\boldsymbol{k}_2,\boldsymbol{k}_3) &= \frac{1}{3}\left[(1-\mu^2_{1,23})\beta(\boldsymbol{k}_2,\boldsymbol{k}_3)+\ \text{(cyclic perm.)}\right],\\
K_{\rm sym}(\boldsymbol{k}_1,\boldsymbol{k}_2,\boldsymbol{k}_3) &= \frac{1}{3}\left[\frac{1}{2}(1-\mu^2_{1,23})\Big\{\alpha(\boldsymbol{k}_2,\boldsymbol{k}_3)+\alpha(\boldsymbol{k}_3,\boldsymbol{k}_3)\Big\}+\ \text{(cyclic perm.)}\right],\\
L_{\rm sym}(\boldsymbol{k}_1,\boldsymbol{k}_2,\boldsymbol{k}_3) &= \frac{1}{3}\left[(1-\mu^2_{1,23})(1-\mu^2_{2,3})+\ \text{(cyclic perm.)}\right],
\end{aligned}
$$

In the expressions (B9) and (B10), new growth functions originating from non-linearity of the Poisson equation appear. The evolution equations for these function are given by

$$
\begin{aligned}
&\widehat{\mathcal{L}}\,C_3 = \dot{D}_1\dot{F}_2,\\
&\widehat{\mathcal{L}}\,I_3 = D_1(\ddot{F}_2+2H\dot{F}_2)+\dot{D}_1\dot{F}_2,\\
&\widehat{\mathcal{L}}\,J_3 = -\frac{r_{\rm c}^2}{6\beta^3}\left(\frac{\kappa\rho_m}{3}\right)^2\frac{D_1^3}{7},\\
&\widehat{\mathcal{L}}\,K_3 = -\frac{r_{\rm c}^2}{6\beta^3}\left(\frac{\kappa\rho_m}{3}\right)^2\frac{5D_1^3}{7},\\
&\widehat{\mathcal{L}}\,L_3 = -\frac{r_{\rm c}^2}{6\beta^3}\left(\frac{\kappa\rho_m}{3}\right)^2 D_1F_2+\frac{r_{\rm c}^4}{9\beta^5}\left(\frac{\kappa\rho_m}{3}\right)^3 D_1^3.
\end{aligned}
$$

2. One-loop power spectra

Using the perturbative solutions obtained above, the power spectrum can be expressed as

$$
P_{ab}(k;t) = P^{(11)}_{ab}(k;t)+P^{(22)}_{ab}(k;t)+P^{(13)}_{ab}(k;t)+\cdots \qquad ; \quad (a,b=\delta \text{ or } \theta). \tag{B11}
$$

The terms $P^{(11)}(k)$ imply the linear power spectrum, given by

$$
P^{(11)}_{\delta\delta}(k;t) = D_1^2(t)\,P_0(k), \quad P^{(11)}_{\delta\theta}(k;t) = -\frac{D_1(t)\dot{D}_1(t)}{H}\,P_0(k), \quad P^{(11)}_{\theta\theta}(k;t) = \left(\frac{\dot{D}_1(t)}{H}\right)^2 P_0(k), \tag{B12}
$$

where the power spectrum $P_0(k)$ is defined by

$$
\langle\delta_0(\boldsymbol{k})\delta_0(\boldsymbol{k}')\rangle = (2\pi)^3\delta_{\rm D}(\boldsymbol{k}+\boldsymbol{k}')\,P_0(|\boldsymbol{k}|). \tag{B13}
$$

The terms $P^{(22)}(k)$ and $P^{(13)}(k)$ are the so-called one-loop power spectra whose explicit expressions respectively become

$$\begin{aligned}P^{(22)}_{\delta\delta}(k;t) &= \frac{k^3}{(2\pi)^2}\int_0^\infty dx\, x^2 P_0(kx)\int_{-1}^{1} d\mu\, P_0\left(k\sqrt{1+x^2-2\mu x}\right)\\ &\quad\times 2\Big[D_1^4(t)\left\{\frac{3x+7\mu-10\mu^2 x}{14x(1+x^2-2\mu x)}\right\}^2 + F_2^2(t)\left(\frac{\mu^2-1}{1+x^2-2\mu x}\right)^2\\ &\quad + D_1^2(t)F_2(t)\,\frac{(3x+7\mu-10\mu^2x)(1-\mu^2)}{7x(1+x^2-2\mu x)^2}\Big],\end{aligned} \tag{B14}$$

$$\begin{aligned}P^{(22)}_{\delta\theta}(k;t) &= \frac{k^3}{(2\pi)^2}\int_0^\infty dx\, x^2 P_0(kx)\int_{-1}^{1} d\mu\, P_0\left(k\sqrt{1+x^2-2\mu x}\right)\\ &\quad\times\Big[-\frac{\dot D_1 D_1^3}{H}\,\frac{(x-7\mu+6\mu^2x)(-3x-7\mu+10\mu^2x)}{98x^2(1+x^2-2\mu x)^2} - \frac{\dot F_2 F_2}{H}\,\frac{2(\mu^2-1)^2}{(1+x^2-2\mu x)^2}\\ &\quad - \frac{\dot F_2 D_1^2}{H}\,\frac{(-3x-7\mu+10\mu^2x)(\mu^2-1)}{7x(1+x^2-2\mu x)^2} - \frac{\dot D_1 D_1 F_2}{H}\,\frac{(x-7\mu+6\mu^2x)(\mu^2-1)}{7x(1+x^2-2\mu x)^2}\Big],\end{aligned} \tag{B15}$$

$$\begin{aligned}P^{(22)}_{\theta\theta}(k;t) &= \frac{k^3}{(2\pi)^2}\int_0^\infty dx\, x^2 P_0(kx)\int_{-1}^{1} d\mu\, P_0\left(k\sqrt{1+x^2-2\mu x}\right)\\ &\quad\times 2\Big[\left(\frac{\dot D_1 D_1}{H}\right)^2\left\{\frac{(x-7\mu+6\mu^2x)}{14x(1+x^2-2\mu x)}\right\}^2 + \left(\frac{\dot F_2}{H}\right)^2\frac{(\mu^2-1)^2}{(1+x^2-2\mu x)^2}\\ &\quad + \frac{\dot D_1 \dot F_2 D_1}{H^2}\,\frac{(x-7\mu+6\mu^2x)(\mu^2-1)}{7x(1+x^2-2\mu x)^2}\Big],\end{aligned} \tag{B16}$$

for $P^{(22)}(k)$, and

$$\begin{aligned}P^{(13)}_{\delta\delta}(k;t) &= \frac{k^3}{(2\pi)^2}P_0(k)\int_0^\infty dx\, P_0(kx)\\ &\quad\times\Big[\, D_1^4(t)\,\frac{1}{252x^3}\Big\{12x-158x^3+100x^5-42x^7+3(x^2-1)^3(7x^2+2)\ln\left|\frac{1+x}{1-x}\right|\Big\}\\ &\quad + D_1(t)C_3(t)\,\frac{1}{6x^3}\Big\{6x-16x^3-6x^5+3(x^2-1)^3\ln\left|\frac{1+x}{1-x}\right|\Big\}\\ &\quad + D_1(t)I_3(t)\,\frac{1}{6x}\Big\{6x+16x^3-6x^5+3(x^2-1)^3\ln\left|\frac{1+x}{1-x}\right|\Big\}\\ &\quad + D_1(t)\left\{K_3(t)+L_3(t)\right\}\,\frac{1}{12x^3}\Big\{-6x+22x^3+22x^5-6x^7+3(x^2-1)^4\ln\left|\frac{1+x}{1-x}\right|\Big\}\Big],\end{aligned} \tag{B17}$$

$$\begin{aligned}P^{(13)}_{\delta\theta}(k;t) &= \frac{k^3}{(2\pi)^2}P_0(k)\int_0^\infty dx\, P_0(kx)\\ &\quad\times\Big[\,-\frac{\dot D_1 D_1^3}{H}\,\frac{1}{252x^3}\Big\{24x-202x^3+56x^5-30x^7+3(x^2-1)^3(5x^2+4)\ln\left|\frac{1+x}{1-x}\right|\Big\}\\ &\quad - \frac{(D_1C_3)^{\cdot}}{H}\,\frac{1}{12x^3}\Big\{6x-16x^3-6x^5+3(x^2-1)^3\ln\left|\frac{1+x}{1-x}\right|\Big\}\\ &\quad - \frac{(D_1I_3)^{\cdot}-\dot F_2 D_1^2}{H}\,\frac{1}{12x}\Big\{6x+16x^3-6x^5+3(x^2-1)^3\ln\left|\frac{1+x}{1-x}\right|\Big\}\\ &\quad - \frac{\{D_1(K_3+L_3)\}^{\cdot}}{H}\,\frac{1}{24x^3}\Big\{-6x+22x^3+22x^5-6x^7+3(x^2-1)^4\ln\left|\frac{1+x}{1-x}\right|\Big\}\Big],\end{aligned} \tag{B18}$$

$$
\begin{aligned}
P^{(13)}_{\theta\theta}(k;t) \;=\; & \frac{k^3}{(2\pi)^2}P_0(k)\int_0^\infty dx\, P_0(kx) \\
& \times\Big[\,\left(\frac{\dot D_1 D_1}{H}\right)^2 \frac{1}{84x^3}\Big\{12x-82x^3+4x^5-6x^7+3(x^2-1)^3(x^2+2)\ln\left|\frac{1+x}{1-x}\right|\Big\} \\
& \quad +\frac{\dot D_1\dot C_3}{H^2}\,\frac{1}{6x^3}\Big\{6x-16x^3-6x^5+3(x^2-1)^3\ln\left|\frac{1+x}{1-x}\right|\Big\} \\
& \quad +\frac{\dot D_1(\dot I_3-\dot F_2 D_1)}{H^2}\,\frac{1}{6x}\Big\{6x+16x^3-6x^5+3(x^2-1)^3\ln\left|\frac{1+x}{1-x}\right|\Big\} \\
& \quad +\frac{\dot D_1(\dot K_3+\dot L_3)}{H^2}\,\frac{1}{12x^3}\Big\{-6x+22x^3+22x^5-6x^7+3(x^2-1)^4\ln\left|\frac{1+x}{1-x}\right|\Big\}\Big], \qquad \text{(B19)}
\end{aligned}
$$

for $P^{(13)}(k)$.

The power spectrum without the non-linear interaction terms $\mathcal{I}$ can be obtained by putting $F_2 = C_3 = I_3 = K_3 = L_3 = 0$ in $P^{(22)}$ and $P^{(13)}$.

[1] S. Nojiri and S. D. Odintsov, ECONF **C0602061**, 06 (2006), hep-th/0601213.
[2] K. Koyama, Gen. Rel. Grav. **40**, 421 (2008), 0706.1557.
[3] R. Durrer and R. Maartens, (2008), 0811.4132.
[4] R. Durrer and R. Maartens, Gen. Rel. Grav. **40**, 301 (2008), 0711.0077.
[5] W. Hu and I. Sawicki, (2007), arXiv:0708.1190 [astro-ph].
[6] J.-P. Uzan and F. Bernardeau, Phys. Rev. **D64**, 083004 (2001), hep-ph/0012011.
[7] A. Lue, R. Scoccimarro, and G. Starkman, Phys. Rev. **D69**, 044005 (2004), astro-ph/0307034.
[8] M. Ishak, A. Upadhye, and D. N. Spergel, Phys. Rev. **D74**, 043513 (2006), astro-ph/0507184.
[9] L. Knox, Y.-S. Song, and J. A. Tyson, Phys. Rev. **D74**, 023512 (2006).
[10] K. Koyama, JCAP **0603**, 017 (2006), astro-ph/0601220.
[11] T. Chiba and R. Takahashi, Phys. Rev. **D75**, 101301 (2007), astro-ph/0703347.
[12] L. Amendola, M. Kunz, and D. Sapone, JCAP **0804**, 013 (2008), 0704.2421.
[13] K. Yamamoto, D. Parkinson, T. Hamana, R. C. Nichol, and Y. Suto, Phys. Rev. **D76**, 023504 (2007), 0704.2949.
[14] K. Yamamoto, T. Sato, and G. Huetsi, Prog. Theor. Phys. **120**, 609 (2008), 0805.4789.
[15] Y.-S. Song and W. J. Percival, (2008), 0807.0810.
[16] M. Kunz and D. Sapone, Phys. Rev. Lett. **98**, 121301 (2007), astro-ph/0612452.
[17] B. Jain and P. Zhang, (2007), 0709.2375.
[18] Y.-S. Song and K. Koyama, JCAP **01**, 048 (2009), 0802.3897.
[19] Y.-S. Song and O. Dore, (2008), 0812.0002.
[20] N. Afshordi, G. Geshnizjani, and J. Khoury, (2008), 0812.2244.
[21] G.-B. Zhao, L. Pogosian, A. Silvestri, and J. Zylberberg, (2008), 0809.3791.
[22] G.-B. Zhao, L. Pogosian, A. Silvestri, and J. Zylberberg, (2009), 0905.1326.
[23] J. M. Alimi *et al.*, (2009), 0903.5490.
[24] H. Oyaizu, Phys. Rev. **D78**, 123523 (2008), 0807.2449.
[25] H. Oyaizu, M. Lima, and W. Hu, Phys. Rev. **D78**, 123524 (2008), 0807.2462.
[26] F. Schmidt, M. V. Lima, H. Oyaizu, and W. Hu, (2008), 0812.0545.
[27] T. P. Sotiriou and V. Faraoni, (2008), 0805.1726.
[28] S. Capozziello and M. Francaviglia, Gen. Rel. Grav. **40**, 357 (2008), 0706.1146.
[29] S. Gottlober, H. J. Schmidt, and A. A. Starobinsky, Class. Quant. Grav. **7**, 893 (1990).
[30] D. Wands, Class. Quant. Grav. **11**, 269 (1994), gr-qc/9307034.
[31] G. Magnano and L. M. Sokolowski, Phys. Rev. **D50**, 5039 (1994), gr-qc/9312008.
[32] J. Khoury and A. Weltman, Phys. Rev. **D69**, 044026 (2004), astro-ph/0309411.
[33] W. Hu and I. Sawicki, Phys. Rev. **D76**, 064004 (2007), 0705.1158.
[34] A. A. Starobinsky, JETP Lett. **86**, 157 (2007), 0706.2041.
[35] S. A. Appleby and R. A. Battye, Phys. Lett. **B654**, 7 (2007), 0705.3199.
[36] G. Cognola, E. Elizalde, S. Nojiri, S. D. Odintsov, L. Sebastiani and S. Zerbini, Phys. Rev. D **77**, 046009 (2008) [arXiv:0712.4017 [hep-th]].
[37] A. Taruya and T. Hiramatsu, Astrophys. J **674**, 617 (2008), 0708.1367.
[38] T. Nishimichi *et al.*, Publ. Astron. Soc. Japan **61**, 321 (2009), 0810.0813.
[39] M. Crocce and R. Scoccimarro, Phys. Rev. **D73**, 063519 (2006), astro-ph/0509418.
[40] P. Valageas, (2006), astro-ph/0611849.

[41] R. Nagata, T. Chiba, and N. Sugiyama, Phys. Rev. **D66**, 103510 (2002), astro-ph/0209140.
[42] G. Esposito-Farese and D. Polarski, Phys. Rev. **D63**, 063504 (2001), gr-qc/0009034.
[43] A. Riazuelo and J.-P. Uzan, Phys. Rev. **D66**, 023525 (2002), astro-ph/0107386.
[44] E. Bertschinger and P. Zukin, Phys. Rev. **D78**, 024015 (2008), 0801.2431.
[45] G. R. Dvali, G. Gabadadze, and M. Porrati, Phys. Lett. **B485**, 208 (2000), hep-th/0005016.
[46] M. A. Luty, M. Porrati, and R. Rattazzi, JHEP **09**, 029 (2003), hep-th/0303116.
[47] T. Tanaka, Phys. Rev. **D69**, 024001 (2004), gr-qc/0305031.
[48] K. Koyama and F. P. Silva, Phys. Rev. **D75**, 084040 (2007), hep-th/0702169.
[49] C. Deffayet, G. R. Dvali, G. Gabadadze, and A. I. Vainshtein, Phys. Rev. **D65**, 044026 (2002), hep-th/0106001.
[50] Y. Fujii and K. Maeda, *Cambridge, USA: Univ. Pr. (2003)*
[51] A. Taruya, T. Nishimichi, S. Saito, and T. Hiramatsu, (2009), 0906.0507.
[52] J. Carlson, M. White, and N. Padmanabhan, (2009), 0905.0479.
[53] T. Hiramatsu and A. Taruya, Phys. Rev. **D79**, 103526 (2009), 0902.3772.
[54] C. Deffayet, Phys. Lett. **B502**, 199 (2001), hep-th/0010186.
[55] V. Sahni and Y. Shtanov, JCAP **0311**, 014 (2003), astro-ph/0202346.
[56] A. Lue and G. D. Starkman, Phys. Rev. **D70**, 101501 (2004), astro-ph/0408246.
[57] K. Koyama, Class. Quant. Grav. **24**, R231 (2007), 0709.2399.
[58] M. Fairbairn and A. Goobar, Phys. Lett. **B642**, 432 (2006), astro-ph/0511029.
[59] R. Maartens and E. Majerotto, Phys. Rev. **D74**, 023004 (2006), astro-ph/0603353.
[60] W. Fang *et al.*, Phys. Rev. **D78**, 103509 (2008), 0808.2208.
[61] K. Koyama and R. Maartens, JCAP **0601**, 016 (2006), astro-ph/0511634.
[62] A. Nicolis, R. Rattazzi, and E. Trincherini, (2008), 0811.2197.
[63] T. Chiba, Phys. Lett. **B575**, 1 (2003), astro-ph/0307338.
[64] S. Nojiri and S. D. Odintsov, Phys. Rev. D **68**, 123512 (2003) [arXiv:hep-th/0307288].
[65] A. V. Frolov, Phys. Rev. Lett. **101**, 061103 (2008), 0803.2500.
[66] T. Kobayashi and K.-i. Maeda, (2008), 0807.2503.
[67] T. Kobayashi and K.-i. Maeda, Phys. Rev. **D79**, 024009 (2009), 0810.5664.
[68] E. Babichev and D. Langlois, arXiv:0904.1382 [gr-qc].
[69] T. Tatekawa and S. Tsujikawa, JCAP **0809**, 009 (2008), 0807.2017.
[70] A. Borisov and B. Jain, (2008), 0812.0013.
[71] We would like to thank Wayne Hu and Fabian Schmidt for providing us data from their N-body simulations.
[72] The Virgo Consortium, R. E. Smith *et al.*, Mon. Not. Roy. Astron. Soc. **341**, 1311 (2003), astro-ph/0207664.
[73] R. Lazkoz, R. Maartens, and E. Majerotto, Phys. Rev. **D74**, 083510 (2006), astro-ph/0605701.
[74] T. Giannantonio, Y.-S. Song, and K. Koyama, Phys. Rev. **D78**, 044017 (2008), 0803.2238.
[75] L. Casarini, A. V. Maccio', and S. A. Bonometto, JCAP **0903**, 014 (2009), 0810.0190.
[76] F. Schmidt, (2009), 0905.0858.
[77] I. Laszlo and R. Bean, Phys. Rev. **D77**, 024048 (2008), 0709.0307.
[78] W. H. Press, S. A. Teukolsky, W. T. Vetterling, and B. P. Flannery, *Numerical Recipes: The Art of Scientific Computing* (Cambridge University Press, 2007).
[79] F. Bernardeau, S. Colombi, E. Gaztanaga, and R. Scoccimarro, Phys. Rept. **367**, 1 (2002), astro-ph/0112551.